

## A novel strategy for triacylglycerides and polyhydroxyalkanoates production using waste lipids

Lucía Argiz, Rebeca González-Cabaleiro, Ángeles Val del Río, Jesús González-López, Anuska Mosquera-Corralla

**Accepted Manuscript**

### **How to cite:**

Science of The Total Environment, 763 (2021), 142944

<https://doi.org/10.1016/j.scitotenv.2020.142944>

### **Copyright information:**

© 2020 Elsevier B.V.

This manuscript version is made available under the CC-BY-NC-ND 4.0 license

(<http://creativecommons.org/licenses/by-nc-nd/4.0/>)

## **A novel strategy for triacylglycerides and polyhydroxyalkanoates production using waste lipids**

Lucía Argiz <sup>a</sup> \*, Rebeca González-Cabaleiro <sup>b</sup>, Ángeles Val del Río <sup>a</sup>, Jesús González-López <sup>c</sup>, Anuska Mosquera-Corral <sup>a</sup>

<sup>a</sup> CRETUS Institute, Department of Chemical Engineering, Universidade de Santiago de Compostela, 15782 Santiago de Compostela, Galicia, Spain

<sup>b</sup> Department of Infrastructure and Environment, University of Glasgow, Rankine Building, Glasgow, G12 8LT, UK

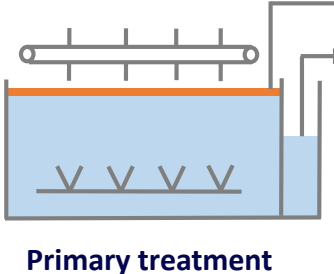
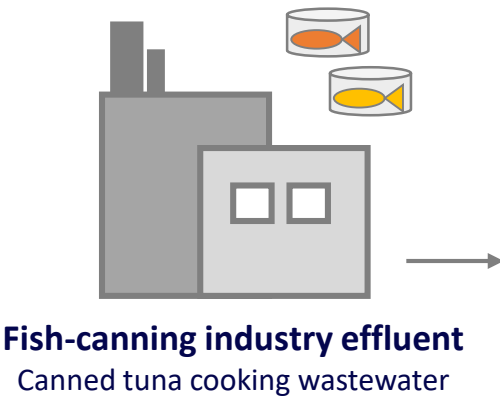
<sup>c</sup> Department of Microbioloy and Institute of Water Research, Universidad de Granada, Granada, Spain

\* Corresponding author: [luciaargiz.montes@usc.es](mailto:luciaargiz.montes@usc.es)

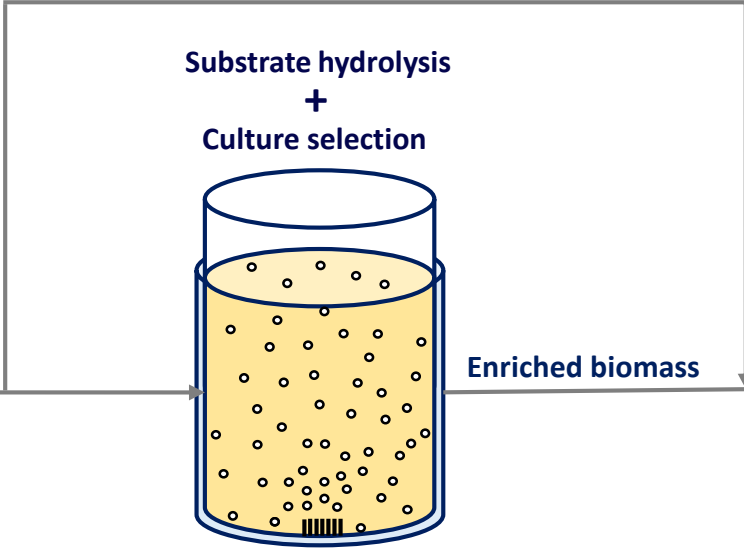
## Highlights

- Preferent triacylglycerides or polyhydroxyalkanoates storage from waste lipids
- No waste oil pretreatment was needed before the enrichment and accumulation stages.
- Dominant metabolic pathways depended on the imposed selective pressures.
- Carbon and nitrogen (limited) uncoupling promoted polyhydroxyalkanoates storage.
- Low pH in the famine, an additional advantage for triacylglyceride-accumulators.

# VALORIZATION PROCESS

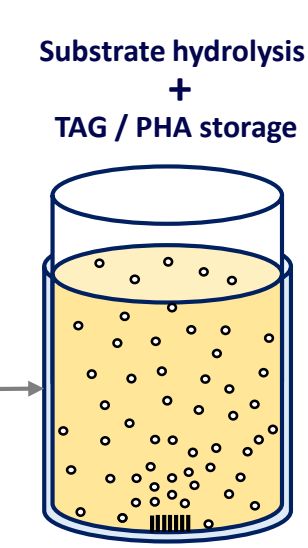


Waste fish oil  
Clarified effluent



**Enrichment SBR**

Enriched biomass



**Accumulation FBR**

Effect of the selection strategy	
Uncoupled C and N feedings	82 wt % PHAs (TAG:PHA 4:96) 0.80 Cmmol PHA / Cmmol oil
Uncoupled C and N feedings Low pH in the famine phase	43 wt % TAGs (TAG:PHA 13:87) 0.67 Cmmol TAG / Cmmol oil

Fed batch reactor (FBR); polyhydroxyalkanoates (PHAs); sequential batch reactor (SBR); triacylglycerides (TAGs)

# 1 **A novel strategy for triacylglycerides and polyhydroxyalkanoates** 2 **production using waste lipids**

3 Lucía Argiz <sup>a</sup>\*, Rebeca González-Cabaleiro <sup>b</sup>, Ángeles Val del Río <sup>a</sup>, Jesús González-López <sup>c</sup>,  
4 Anuska Mosquera-Corral <sup>a</sup>

5 <sup>a</sup> CRETUS Institute, Department of Chemical Engineering, Universidade de Santiago de  
6 Compostela, 15782 Santiago de Compostela, Galicia, Spain

7 <sup>b</sup> Department of Infrastructure and Environment, University of Glasgow, Rankine Building,  
8 Glasgow, G12 8LT, UK

9 <sup>c</sup> Department of Microbiology and Institute of Water Research, Universidad de Granada,  
10 Granada, Spain

11

12 \* Corresponding author: [luciaargiz.montes@usc.es](mailto:luciaargiz.montes@usc.es)

13

## 14 **ABSTRACT**

15 Lipids are one of the main components of the organic matter present in the effluents of the food-  
16 processing industry. These waste streams can be biotransformed into valuable triacylglycerides (TAGs)  
17 and polyhydroxyalkanoates (PHAs), precursors of biofuels and biomaterials alternative to petroleum-  
18 based products. These compounds are yielded by mixed microbial cultures, and considering that both  
19 TAG and PHA accumulators may coexist within the community, it seems crucial to define those  
20 operational strategies that might control the selection of the dominant metabolic pathways (TAG or PHA  
21 accumulation). In this work, residual fish-canning oil was used as a carbon source in a two-stage process  
22 (culture selection and intracellular compounds accumulation) in which the substrate was simultaneously  
23 hydrolyzed in these two stages without the need for a previous fermentation unit. It was pretended to  
24 maximise preferential TAG or PHA storage in the accumulation reactor by the imposition of certain  
25 selective pressures in the enrichment one. Uncoupling C and N feedings and limiting nitrogen availability  
26 in the medium, allowed to maximise PHA production (82.3 wt % of PHAs, 0.80 Cmmol<sub>PHA</sub>/Cmmol<sub>S</sub>).  
27 Besides, when low pH in the famine phase was considered as additional selective pressure, it was possible  
28 to shift the ratio TAG:PHA from 4:96 obtaining 43.0 wt % of TAGs (0.67 Cmmol<sub>TAG</sub>/Cmmol<sub>S</sub>).  
29 Therefore, this novel and simplified process demonstrated versatility and efficiency in the storage of  
30 TAGs and PHAs from a unique residual feedstock and using an open culture proving that product  
31 selection can be harnessed if choosing the right operational conditions in the enrichment stage.

32

33 **Keywords:** biotransformation; lipidic waste; mixed microbial culture; pH; uncoupled feeding.

34

- 35 ADF: aerobic dynamic feeding
- 36 C: carbon
- 37 COD: chemical oxygen demand
- 38 DO: dissolved oxygen (mg/L)
- 39 FBR: fed-batch reactor
- 40 F/F: feast/famine
- 41 FFA: free fatty acids
- 42 MMC: mixed microbial culture
- 43 N: nitrogen
- 44 PHA: polyhydroxyalkanoate
- 45  $q_N$ : maximum specific nitrogen consumption rate ( $C_{mmolN}/C_{mmolX}\cdot h$ )
- 46  $q_{PHA}$ : maximum specific polyhydroxyalkanoates production rate
- 47 ( $C_{mmolPHA}/C_{mmolX}\cdot h$ )
- 48  $q_S$ : maximum specific carbon consumption rate ( $C_{mmolS}/C_{mmolX}\cdot h$ )
- 49  $q_{TAG}$ : maximum specific triacylglycerides production rate ( $C_{mmolTAG}/C_{mmolX}\cdot h$ )
- 50  $q_X$ : maximum specific active biomass production rate ( $C_{mmolX}/C_{mmolS}\cdot h$ )
- 51 S: substrate
- 52 SBR: sequencing batch reactor
- 53 TAG: triacylglyceride
- 54 TN: total nitrogen (mg/L)
- 55 TS: total solids (g/g)

- 56 TSS: total suspended solids (g/L)
- 57 VS: volatile solids (g/g)
- 58 VSS: volatile suspended solids (mg/L)
- 59 WWTP: wastewater treatment plant
- 60 X: active biomass (Cmmol/L)
- 61  $Y_{\text{PHA}}$ : maximum polyhydroxyalkanoates production yield (Cmmol<sub>PHA</sub>/Cmmol<sub>S</sub>)
- 62  $Y_{\text{TAG}}$ : maximum triacylglycerides production yield (Cmmol<sub>TAG</sub>/Cmmol<sub>S</sub>)
- 63  $Y_{\text{X}}$ : maximum active biomass production yield(Cmmol<sub>X</sub>/Cmmol<sub>S</sub>)
- 64

## 65 **1. INTRODUCTION**

66 The food industry generates large volumes of solid and liquid waste types that suppose  
67 a significant environmental and economic concern. Among the industries causing a  
68 global major impact are seafood and fish-processing activities (Kosseva, 2013).  
69 Specifically, the fish-canning industry is characterized by the generation of large  
70 amounts of high strength liquid effluents (Cristóvão et al., 2015), which are rich in  
71 lipids, one of the main components of natural fish (Chipasa and Mędrzycka, 2006).  
72 These effluents are usually pre-treated before biological treatment, to separate solids  
73 and lipids using different physicochemical processes (Ahmad et al., 2020). Then, lipids  
74 are commonly composted or anaerobically digested (Cristóvão et al., 2015; Tamis et al.,  
75 2015). However, with the advancement of science and technology, wastewater  
76 treatment methods are constantly improving (Wu et al., 2020). In the last years,  
77 industrial waste fish oils have been identified as potential feedstocks for the obtention of  
78 value-added compounds such as renewable 2<sup>nd</sup> generation biofuels (Sawangkeaw and  
79 Ngamprasertsith, 2013) or bioplastics (Surendran et al., 2020), which would contribute  
80 to cope with fossil fuel depletion and environmental problems (Leng et al., 2020).

81 Using single-cell microorganisms, the valorisation of waste oils is feasible since they  
82 are capable of storing important percentages of high-quality compounds that serve as  
83 raw materials or intermediates for a variety of applications (Garay et al., 2014; Gujjala  
84 et al., 2019). Special emphasis is given to triacylglycerides (TAGs) and  
85 polyhydroxyalkanoates (PHAs), excellent reserve materials that constitute the main  
86 compounds accumulated in eukaryotes and prokaryotes, respectively (Revellame et al.,  
87 2012). Their storage fulfils several roles in microorganisms such as cell growth and  
88 division (Garay et al., 2014), stress response against the pressure exerted by certain  
89 environments (Kumar et al., 2018), and energy reserve (Kumar et al., 2020).

90 Fungi and yeast are oleaginous microbes in their majority as they can accumulate over  
91 20 wt % of intracellular TAGs (Alvarez and Steinbüchel, 2003). However, TAGs are  
92 not a common storage compound in bacteria and their accumulation was only described  
93 in a few prokaryotic species belonging to the actinobacterial group (Gujjala et al.,  
94 2019). Bacteria typically biotransform lipids into PHAs (Garay et al., 2014) although  
95 certain species are able to synthesize PHA and TAG together, as it is the case of  
96 *Rhodococcus Ruber* (Alvarez and Steinbüchel, 2003; Garay et al., 2014).

97 Although research on TAG and PHA production from lipidic feedstocks was  
98 traditionally focused on the use of edible plant oils as substrates and pure cultures with  
99 very high accumulation capacity (Basnett et al., 2018; Donot et al., 2014; Pérez-Arauz  
100 et al., 2019), the high production costs, mainly associated with substrate acquisition and  
101 culture conditions pushed for the development of cost-effective alternatives. These  
102 involved the use of waste feedstocks and mixed microbial cultures (MMCs) (Sabapathy  
103 et al., 2020) and not only reduced the costs of the process, but also increased resource  
104 efficiency and improved waste management performance contributing to the  
105 establishment of a circular economic model (Surendran et al., 2020; Yadav et al., 2020).  
106 Recently, it was developed studies regarding the use of animal fats for TAG (Lopes et  
107 al., 2018) and PHA (Sangkharak et al., 2020; Van Thuoc et al., 2019) production using  
108 pure cultures. Regarding MMCs, to the best of the author's knowledge, only the use of  
109 vegetable oils was explored so far. TAG accumulation has been demonstrated feasible  
110 through a two-stage process: (1) selection and enrichment of the MMC; and (2)  
111 maximization of the TAG storage before its extraction and purification (Tamis et al.,  
112 2015). In the case of PHA production, it has been proposed an analogous configuration  
113 that included a previous fermentation of the lipids contained in the residual streams

114 used as a substrate to obtain soluble organic acids (Campanari et al., 2014; Waller et al.,  
115 2012).

116 One of the most common enrichment strategies for PHA production in MMCs is the  
117 aerobic dynamic feeding (ADF), which was also demonstrated to provide a competitive  
118 advantage for TAG accumulators (Tamis et al., 2015). This strategy consists in the  
119 application of subsequent aerobic feast/famine (F/F) cycles in which the culture is  
120 initially subjected to an excess of carbon source and then submitted to carbon  
121 deficiency. Several variations of this enrichment strategy have been tested to optimize  
122 PHA production (Kourmentza et al., 2017). Uncoupling carbon (C) and nitrogen (N)  
123 availability in addition to the F/F regime was demonstrated to cause a positive impact in  
124 PHA accumulation (Lorini et al., 2020; Oliveira et al., 2017; Silva et al., 2017). These  
125 strategies favour its storage in the feast phase (exogenous C availability and N absence  
126 limiting, in turn, the development of non-accumulating microorganisms) and enhance  
127 the growth of populations with high PHA-storage ability in the famine (intracellular C  
128 and external N are available) (Oliveira et al., 2017; Silva et al., 2017). Variations in the  
129 ADF strategy to maximize TAG storage have not been reported yet. However,  
130 Santamauro et al. (2014) considered the possibility of using low pH combined with low  
131 temperature or high salinity to enrich an open culture in extremophile oleaginous  
132 microorganisms. But although it is known that oleaginous microorganisms can thrive  
133 relatively well in low pH environments (Donot et al., 2014), other species might be also  
134 selected under these conditions.

135 In the present research, it was pretended to valorise a residual fish-canning oily stream  
136 for the production of TAGs or PHAs using the same configuration, a two-stage process  
137 consisting of culture selection plus intracellular compounds accumulation in the  
138 enriched culture. Firstly, it was evaluated the feasibility of using the considered waste

139 stream as a substrate. Then, the versatility and robustness of the process were assessed  
140 by providing the most suitable operational conditions (N feeding strategy and pH) that  
141 promoted the follow-up of those metabolic routes concerning the accumulation of TAGs  
142 or PHAs, and hence the preferent development of TAG or PHA producers. Finally, it  
143 was determined the effect of the enrichment strategy over the process productivity and  
144 type of intracellular compounds accumulated.

145

## 146 **2. MATERIALS AND METHODS**

### 147 **2.1. Substrate characteristics and metabolism**

148 The substrate used in this study was residual oil from the cooking water of the industrial  
149 production of canned tuna (Table 1) removed in the primary treatment of the factory  
150 wastewater treatment plant (WWTP). It was characterized by high hydrophobicity  
151 identifying oleic and linoleic as the main fatty acids in its composition with a lower  
152 concentration of palmitic and stearic acids. These, have been previously found as the  
153 main fatty acids of several commercially available tuna products, especially the ones  
154 that are oil-packaged (Maqbool et al., 2011).

155 The residual oil used as a substrate was fed to a MMC in which different routes could  
156 be possible depending on the medium conditions due to the diversity of microorganisms  
157 potentially present in open cultures. The microbial conversion of non-soluble fats and  
158 oils is complex and starts with initial extracellular hydrolysis catalysed by lipases that  
159 yield free fatty acids (FFA) and glycerol. Soluble FFA are then available to be  
160 transported into the cell and once the substrate is taken up, a wide diversity of metabolic  
161 pathways are feasible (Becker, 2010; Garay et al., 2014; Jimenez-diaz et al., 2019;  
162 Tamis et al., 2015). FFA can directly support cell growth but under excess of carbon

163 and especially if a key nutrient is limited (typically nitrogen), certain microorganisms  
164 stop replication processes and utilize the available carbon to synthesize and store  
165 intracellular value-added compounds (Garay et al., 2014). On the one hand, certain  
166 oleaginous microorganisms can accumulate oils in the form of lipid droplets via the *ex*  
167 *novo* pathway when using a hydrophobic substrate (Patel and Matsakas, 2019) such as  
168 the waste fish oil considered in this research work. This metabolic route differs from the  
169 *de novo* pathway, which involves the consumption of hydrophilic substrates, in that it is  
170 entirely independent of nitrogen exhaustion in the medium since lipid accumulation and  
171 cell growth occur simultaneously (Huang et al., 2017). On the other hand, PHA  
172 producers can employ FFA as a substrate for the production of intracellular PHAs via  $\beta$ -  
173 Oxidation pathway (Jimenez-diaz et al., 2019) (Figure 1).

## 174 **2.2 Experimental set-up**

175 For the valorisation of the residual fish-canning oily stream, a two-unit process was  
176 considered: (1) a sequencing batch reactor (SBR) for the enrichment of the MMC and  
177 (2) a fed-batch reactor (FBR) to maximize the production of TAGs and PHAs. In both  
178 units, the substrate was simultaneously hydrolyzed not requiring a prior fermentation  
179 unit.

### 180 **2.2.1 Selection of microorganisms with high accumulation capacity**

181 The SBR for the enrichment of the MMC was inoculated with activated sludge from an  
182 urban WWTP. This unit consisted of a 4-L jacketed glass reactor aerobically operated as  
183 SBR under the F/F regime. Continuous aeration, provided by a couple of diffusers  
184 located at the bottom of the reactor, guaranteed the complete mixture of the system. The  
185 temperature was maintained at  $30 \pm 3$  °C through a thermostatic bath (Techne Inc,  
186 USA). The pH was only controlled off-line by  $\text{NaHCO}_3$  buffer addition.

187 The SBR was operated in cycles of 12 h. After finishing each cycle, half of its total  
188 volume (2 L) was exchanged resulting in hydraulic and solid retention times of 24 h. In  
189 each cycle, 2 mL (equivalent to 114.5 Cmmol) of carbon source were added at the  
190 beginning. The 2 L of dilution water were added at different times depending on the  
191 feeding strategy (Figure S1). This stream contained: 0.60 g/L NH<sub>4</sub>Cl, 0.70 g/L KH<sub>2</sub>PO<sub>4</sub>,  
192 0.14 g/L MgSO<sub>4</sub>, 0.10 g/L KCl, 0.65 – 1.00 g/L KH<sub>2</sub>PO<sub>4</sub>, 2 mL/L of a trace element  
193 solution (Vishniac and Santer, 1957), and 0.0025 g/L allylthiourea to prevent  
194 nitrification. In the uncoupled configurations, nitrogen was added separately as 20 mL  
195 of a concentrated NH<sub>4</sub>Cl solution, reducing the concentration of KH<sub>2</sub>PO<sub>4</sub> in the dilution  
196 water in the same proportion as the NH<sub>4</sub>Cl added.

### 197 **2.2.2 Accumulation of storage compounds**

198 The storage capacity of the enriched culture was assessed by the performance of several  
199 accumulation assays in a 4-L FBR inoculated with the effluent of the SBR. This  
200 bioreactor was operated under the same conditions as those of the SBR except for the  
201 feeding regime. To maximize the accumulation and prevent bacterial growth, no  
202 nitrogen source was fed. The residual oil used as a substrate was added in pulses of 0.80  
203 mL (45.8 Cmmol) following the dissolved oxygen (DO) concentration profile. The  
204 maximum accumulation capacity was assumed when DO concentration remained at  
205 saturation values after adding a substrate pulse (end of the experiment). The pH was  
206 periodically measured and adjusted, if necessary, by adding different volumes of an 18  
207 g/L NaHCO<sub>3</sub> solution.

### 208 **2.2.3 Operational strategy**

209 The SBR for the enrichment of the MMC was operated for 331 days with its operation  
210 subdivided into five periods (I – V). During the whole operation six accumulation  
211 assays in the FBR were performed (days 120, 176, 218, 245, 287, and 322) (Figure S2).

212 In the SBR, C and N were fed together at the beginning of the operation (period I, start-  
213 up – day 203). Afterward, two uncoupled C and N feeding strategies were tested: type A  
214 and B, in periods II (days 204 – 224) and III (days 225 – 251) respectively. In period IV  
215 (days 252 – 307), the pH was considered as an additional selective pressure in the SBR  
216 and finally, in period V (days 308 – end of the operation) the capacity of the system to  
217 recover the conditions of period III was explored. The coupled feeding configuration  
218 comprised the following stages: 1) feeding 2 mL of oil and 2 L of dilution water  
219 containing N (5 min); 2) aerobic reaction (708 min), and 3) 2 L of effluent withdrawal  
220 (7 min). The first uncoupling strategy (type A) consisted of 1) feeding 2 mL of oil (5  
221 min); 2) aerobic reaction (180 min); 3) feeding 2 L of dilution water containing N (5  
222 min); 4) aerobic reaction (523); and 5) effluent withdrawal (7 min). The other  
223 uncoupled configuration tested (type B) involved: 1) feeding 2 mL of oil and 2 L of  
224 dilution water without N (5 min); 2) aerobic reaction (120 – 180 min); 3) feeding 20 mL  
225 of a concentrated solution of N (5 min); 4) aerobic reaction (463 – 583 min); and 5)  
226 effluent withdrawal (7 min) (Figure S1). The length of the aerobic reaction before N  
227 addition was initially established according to the feast length previous to the system  
228 uncoupling and modified when necessary.

### 229 **2.3. Sampling and analysis**

230 For monitoring the SBR operation, the effluent discharged at the end of each cycle and  
231 the dilution water were analysed. Samples for solid-phase analysis were also taken at  
232 the end of the feast phase to determine the evolution of the TAGs and PHAs  
233 accumulated. The operation cycles were periodically characterized, and samples were  
234 taken in the 12 h of cycle operation. The accumulation assays performed in the FBR  
235 were also monitored and samples were taken before the addition of each pulse of  
236 substrate.

237 Temperature and DO concentration were measured on-line using a portable multimeter  
238 (HQ40d, Hach-Lange, USA). The raw samples of the SBR and FBR bioreactors were  
239 characterised on pH (pH and Ion-Meter GLP 22, Crison, Spain), total and volatile  
240 suspended solids (TSS and VSS, respectively) and also in the total chemical oxygen  
241 demand (COD) (APHA/AWWA/WEF, 2017). The COD of the supernatant obtained  
242 after single centrifugation of the samples was also determined (Centrifuge 5430  
243 Eppendorf, USA). In the soluble fraction, after both centrifugation and filtration (0.45  
244 µm pore size, cellulose-ester membrane, Advantec, Japan), soluble chemical oxygen  
245 demand (APHA/AWWA/WEF, 2017), lactic acid (measured by high-performance  
246 liquid chromatography, HP 1100 Agilent Technologies with RI detector 107 7A, USA),  
247 and total nitrogen (TN) were measured (TOC-L analyzer with the TNM- module, TOC-  
248 5000 Shimadzu, Japan). The dilution water was characterised on pH, TN, total organic  
249 carbon ,and inorganic carbon (TOC-L analyzer with the TNM- module, TOC-5000  
250 Shimadzu, Japan). For the substrate characterization, the conductivity was determined  
251 with a portable conductivity meter (probe Sension + EC5 HACH, Spain), lipids were  
252 measured by the Soxhlet extraction method (Soxhlet extractor Jp Selecta 8001800,  
253 Spain) (APHA/AWWA/WEF, 2017) and the elemental composition was determined in  
254 an elemental analyser (FlashEA 1112 Thermo Scientific, USA). Total and volatile  
255 solids (TS and VS, respectively) were measured according to APHA/AWWA/WEF  
256 (2017).

257 Identification and quantification of storage compounds were carried according to the  
258 method described by Fra-Vázquez et al. (2018). For that purpose, fresh biomass samples  
259 were taken, centrifuged (Centrifuge 5430 Eppendorf, USA), frozen, and lyophilized to  
260 obtain a solid phase. Commercial calibration standards of TAGs and PHAs were used:  
261 palmitic-, stearic-, oleic- and linoleic acids, and a copolymer containing 88 %

262 hydroxybutyrate and 12 % hydroxyvalerate (Sigma Aldrich, USA). The monomer  
263 propyl esters were analysed by gas chromatography (HP innovax column equipped with  
264 a FID, Agilent, USA).

#### 265 **2.4 Calculations and statistical analysis**

266 The percentage of intracellular compounds accumulated (TAGs or PHAs) expressed in  
267 dry weight (wt %), was calculated by dividing the measured mass of TAGs or PHAs by  
268 the mass of VSS present in the medium (in grams). Active biomass (X) was estimated  
269 as the difference between the measurements of VSS and storage compounds  
270 accumulated (TAG + PHA). The elemental composition of the biomass was assumed to  
271 be  $\text{CH}_{1.8}\text{O}_{0.5}\text{N}_{0.2}$ .

272 Maximum specific conversion rates of carbon ( $-q_s$ ,  $\text{Cmmol}_s/(\text{Cmmol}_X \cdot \text{h})$ ) and nitrogen  
273 ( $-q_N$ ,  $\text{Cmmol}_N/(\text{Cmmol}_X \cdot \text{h})$ ) consumption, and TAG ( $q_{\text{TAG}}$ ,  $\text{Cmmol}_{\text{TAG}}/(\text{Cmmol}_X \cdot \text{h})$ )  
274 and PHA production ( $q_{\text{PHA}}$ ,  $\text{Cmmol}_{\text{PHA}}/(\text{Cmmol}_X \cdot \text{h})$ ), were determined using the  
275 maximum slopes of the experimental data divided by the active biomass. Similarly, the  
276 specific biomass production rate was determined from the maximum slope of the  
277 produced biomass divided by the amount of substrate fed ( $q_X$ ,  $\text{Cmmol}_X/(\text{Cmmol}_s \cdot \text{h})$ ).  
278 The production yield of the storage compounds ( $Y_{\text{TAG}}$   $\text{Cmmol}_{\text{TAG}}/\text{Cmmol}_s$ ; and  $Y_{\text{PHA}}$ ,  
279  $\text{Cmmol}_{\text{PHA}}/\text{Cmmol}_s$ ) and the biomass ( $Y_X$ ,  $\text{Cmmol}_X/\text{Cmmol}_s$ ) were determined by  
280 dividing the related production rate ( $\text{Cmmol}_{\text{TAG}}/\text{h}$ ,  $\text{Cmmol}_{\text{PHA}}/\text{h}$ , and  $\text{Cmmol}_X/\text{h}$ ) by the  
281 carbon source consumption rate ( $\text{Cmmol}_s/\text{h}$ ).

282 Statistical analysis was performed by SPSS software, IBM Corp Released 2017 (IBM  
283 SPSS Statistics for Windows, Version 25.0 Armonk, NY). One-way variance analysis  
284 (ANOVA) was used to test the existence of statistically significant differences between  
285 the composition of the intracellular compounds accumulated in the SBR during the  
286 different operational periods (five independent groups). To determine which of these

287 groups differed from each other, the Turkey post hoc test was applied. On the other  
288 hand, to compare the type of intracellular compounds accumulated in SBR and FBR  
289 reactors during the same operational periods (comparison of two unrelated groups on  
290 the same dependent variable), the independent-samples t-test was considered. A 5 %  
291 significance level was assumed in both cases.

292

### 293 **3. RESULTS AND DISCUSSION**

#### 294 **3.1 Feasibility of using fish-canning oil to enrich a MMC in TAG and PHA** 295 **producers**

296 During the first 203 days (Period I), the SBR was operated under a coupled feeding  
297 strategy (simultaneous C and N addition) to enrich conventional activated sludge in  
298 microorganisms with high storage ability. It is known that lipids, especially long-chain  
299 fatty acids with saturated carbon chains, are less responsive to biodegradation than other  
300 organic substrates (Chipasa and Mędrzycka, 2006). However, the typical F/F profile  
301 was observed after 3 enrichment cycles (Figure S3.a), which indicated that the culture  
302 was able to consume the substrate despite its high hydrophobicity and organic matter  
303 composition (Table 1).

304 The operation of the reactor became stable after 50 days. During this period, the feast  
305 phase length presented wide variability (from 1.3 to 5.5 hours), and the VSS  
306 concentration sharply decreased due to culture selection (from  $2.13 \pm 0.10$  g/L to  $0.32 \pm$   
307  $0.04$  g/L between days 1 and 44). From day 45 onwards, the length of the feast phase  
308 followed a downward trend and reduced its variability. Nevertheless, even after more  
309 than 100 days it still ranged between 2 to 4 hours (feast/cycle ratio of  $0.21 \pm 0.07$ ).  
310 According to Dionisi et al. (2005), ratios lower than approximately 0.25 allow for the  
311 selection of microorganisms with a good storage ability. These variations in the feast

312 phase length could be due to the low solubility of the substrate and grease accumulation  
313 in the walls of the reactor, which diffculted mass transfer and limited the microbial  
314 uptake.

315 The pH was maintained close to neutrality (Figure S3.b) by NaHCO<sub>3</sub> addition in the  
316 dilution water. With the progress of the operation, NaHCO<sub>3</sub> addition was reduced (from  
317 1 to 0.64 g/L) until reaching stationary state. Occasionally, excess of NaHCO<sub>3</sub> increased  
318 the pH in the liquid bulk above neutral (e.g. on day 50 of operation, 0.7 g/L NaHCO<sub>3</sub>  
319 were added in the feeding, and a pH of 7.9 was observed at the end of the cycle) (Figure  
320 S3.c). In these conditions, the FFA produced in a first hydrolysatation of the substrate by  
321 lipase-catalysed reactions, saponified and became unavailable for microbial  
322 metabolization. Once the pH was optimised, the possible saponification did not occur  
323 anymore. Although after feeding, the pH slightly increased during the feast (e.g. from  
324 7.0 to 7.4 on day 72 and from 7.0 to 7.3 on day 171), it decreased to the initial values  
325 remaining almost constant during the whole cycle in period I (Figure 2.a, 2.b and 2.c).

326 In period I, the ratio C/N was maintained at  $16.7 \pm 2.4$  g COD/g TN, and about  $274 \pm 28$   
327 g of TN were fed in each cycle. Neither the COD nor the TN were fully consumed  
328 during the SBR cycle and average concentrations of  $162 \pm 40$  mg COD/L (measured in  
329 the centrifuged and non-filtered sample) and  $81 \pm 17$  mg TN/L were detected in the  
330 effluent (end of the cycle). All the consumed nitrogen was assumed to be used for  
331 growth since nitrification was inhibited by allylthiourea addition. The presence of  
332 remnant COD at the end of each cycle is explained by the nature of the substrate and the  
333 presence of slowly biodegradable or recalcitrant compounds. The composition of the  
334 substrate and in special its hydrophobicity (slow diffusion) could have limited microbial  
335 growth (as no N limiting conditions were imposed) and explain the low VSS  
336 concentrations obtained at steady-state,  $0.58 \pm 0.06$  g/L (Figure S3.d).

337 During the feast phase of period I, microbial growth due to extracellular substrate  
338 consumption, along with intracellular accumulation was observed (Figure 2.a, 2.b and  
339 2.c), but the progressive enrichment of the culture enhanced the use of intracellular  
340 substrate for growth during the famine phase. For example, on day 50, microorganisms  
341 grew during the feast while 13.7 wt % TAGs and 0.9 wt % PHAs was accumulated and  
342 no significant growth was observed during the famine phase (Table 2). However, once  
343 these percentages increased on day 78 up to 20.6 wt % and 1.6 wt %, respectively,  
344 growth took place during both phases (Table 2).

345 The percentage of intracellular compounds accumulated (as a sum of PHAs and TAGs)  
346 did not significantly vary after day 78 onwards (period I), although changes in the  
347 composition were observed, which suggested alterations in the cellular metabolism due  
348 to a slight enrichment of the culture in PHA-accumulators (Silva et al., 2017). For  
349 example, on day 171 the highest PHA production (5.3 wt %) was reached in period I but  
350 concomitantly, TAGs accumulated decreased (10.8 wt %) in comparison with days 78,  
351 111, and 118 (Figure 3.a).

352 Results obtained in period I showed the feasibility of the culture to metabolize the fish-  
353 canning waste oil. However, the carbon source was mainly used for growth as a  
354 consequence of the high N availability present in the medium. Once the substrate was  
355 hydrolyzed, FFA weretransported into the cell and mainly degraded for biomass  
356 production (respiration via the Krebs Cycle) (Figure 1). At the same time, part of the  
357 FFA were directly accumulated as lipid reserve (TAGs with a composition proportional  
358 to that of the substrate (Table 1, Table 2)) via the *ex novo* fatty acids pathway (Figure  
359 1), a primary anabolic process occurring simultaneously with the production of lipid-  
360 free biomass regardless of the C/N ratio in the medium (Carsanba et al., 2018; Lopes et  
361 al., 2018; Pérez-Arauz et al., 2019;). Besides, results obtained in period I (Table 2)

362 evidenced that the presence of too high N concentrations blocked PHA biosynthesis, 3-  
363 Hydroxyacyl-CoA instead of being polymerized, was further transformed into acetyl-  
364 CoA and channelled into the Krebs cycle (Figure 1) (Tan et al., 2014).  
365 Consequently, the enrichment stage of the process needed to be optimized to improve  
366 culture selection and maximize TAG or PHA storage.

### 367 **3.2 Optimization of the SBR enrichment strategy**

368 In this section, shifts in the SBR enrichment strategy were explored to improve  
369 selection and establish the operational conditions for the preferential development of  
370 TAG or PHA-storing populations. Thus, although both storage compounds are  
371 considered valuable potential sources (Garay et al., 2014), their mixture seems not and  
372 might hinder downstream extraction and purification processes.

#### 373 **3.2.1 Channelling lipids metabolism towards PHA production**

##### 374 **3.2.1.1 Nitrogen availability limitation**

375 In periods II and III, N availability was limited during the feast phase (unbalanced  
376 nutrient conditions) to favour the PHA accumulation pathway (Figure 1) and maximise  
377 PHA storage (Tan et al., 2014). For that purpose, two different strategies were tested in  
378 the SBR and its cycle configuration was changed on day 204 to set uncoupling type A,  
379 (period II) and on day 225 to set uncoupling type B (period III). In both cases, C and N  
380 feedings were uncoupled to supply the N source at the end of the feast ensuring  
381 unbalanced nutrient conditions (C excess in the presence of N limitation). The amount  
382 of N added was limited to the minimum needed for microbial growth. Therefore, N was  
383 controlled maintaining a minimum concentration in the effluent of the SBR. The  
384 quantity of TN added was reduced from  $274 \pm 28$  to  $141 \pm 10$  g of TN per cycle, and  
385 consequently, about  $12 \pm 4$  mg TN/L were measured in the effluent, which supposed a  
386 reduction of more than 85 % respect to the values observed in the coupled

387 configuration. After modifying the N feeding strategy, specific nitrogen consumption  
388 and biomass production rates were substantially lower during the feast phase when  
389 compared with period I, especially in the case of the type B configuration (period III)  
390 (Table 2). In periods II and III, the specific N consumption rate significantly decreased  
391 during the feast phase and biomass growth mainly occurred in the famine phase,  
392 favouring culture selection (Table 2). Consequently, a positive effect over PHA  
393 accumulation was observed (Figure 3.a), which confirmed that N limitation and C and  
394 N uncoupling allowed for lipids biotransformation into PHAs and promoted the  
395 enrichment of the culture in PHA producers.

396 After C and N uncoupling, the ratio between the feast phase length and the length of the  
397 whole cycle decreased (Figure S3.a). This result evidenced the enrichment of the  
398 microbial culture in species with high storage ability (Dionisi et al., 2005). The ratio  
399 was reduced from  $0.21 \pm 0.07$  in period I (coupled system, accumulation + extracellular  
400 growth), to  $0.10 \pm 0.05$  and  $0.11 \pm 0.04$  in periods II and III (single accumulation).

401 The F/F profile also changed when C and N were uncoupled. Initially, microorganisms  
402 used organic matter as an electron donor and oxygen as an acceptor (DO concentration  
403 decreased). But after this, a lag phase was observed where DO concentration  
404 progressively increased. Then, the addition of nutrients reduced the DO again because  
405 of respiration for microbial growth. Therefore, the DO profiles presented two slopes,  
406 although when the feast length was too short they overlapped (similar DO profiles were  
407 observed by Lorini et al. (2020)). The sum of both slopes showed that accumulation  
408 plus intracellular growth ( $0.35 \pm 0.07$  and  $0.35 \pm 0.06$  in periods II and III, respectively)  
409 took longer than simultaneous accumulation and extracellular growth ( $0.21 \pm 0.07$ ,  
410 period I) (which is in agreement with the observed by Silva et al. (2017) and Oliveira et  
411 al. (2017)) (Figure S4).

### 412 **3.2.1.2 Initial carbon availability**

413 The higher C availability at the beginning of the cycle in the case of the uncoupling type  
414 A cycle (equal amount of COD added in half of the volume) lead to differences in  
415 composition and amount of storage compounds accumulated between the two  
416 uncoupling strategies tested (Figure 3.a; Table 2).

417 During the feast phase, uncoupling type B cycle caused the enhancement of PHA  
418 accumulation at the expense of TAGs (32.1 wt % PHAs and 5.8 wt % TAGs on day  
419 238) in comparison to the uncoupling type A cycle (18.4 wt % PHAs and 25.8 wt %  
420 TAGs on day 218). The total quantity of storage compounds accumulated at the end of  
421 the feast was lower in type B for similar food to microorganism ratios (values of 4.4 and  
422 4.6 g COD/g VSS for A and B, respectively). In the uncoupling strategy A, 22.6 wt %  
423 TAGs and 2.12 wt % PHAs remained at the end of the cycle whereas in type B only 8.0  
424 wt % TAGs and 0.48 wt % PHAs were measured. The higher carbon availability might  
425 be selecting for microorganisms that consume it faster, using shorter pathways, which  
426 could explain the higher TAG than PHA accumulation at the end of the feast phase in  
427 period II. Moreover, due to the high initial concentration in the feast phase, extracellular  
428 carbon was not fully consumed and therefore, it was also available in the famine phase.  
429 This explains the high percentage of TAGs accumulated measured at the end of the  
430 cycle (Vasiliadou et al., 2018).

431 The strategy of uncoupling type B seems to be the most efficient to maximize PHA  
432 production. It favours a higher PHA storage during the feast and avoids the presence of  
433 extracellular substrate during the famine limiting the growth of non-storing populations.

434

435

436

### 437 **3.2.2 Channelling lipids metabolism towards TAG production**

438 The pH was maintained stable during the SBR cycles at almost neutral values during  
439 period I (Figure 2.a, 2.b and 2.c) showing an average of  $7.1 \pm 0.3$  at the end of the cycle.  
440 However, after uncoupling, this parameter became unstable. In period II (uncoupling A)  
441 the pH decreased but it was recovered by  $\text{NaHCO}_3$  addition (Figure 2.d) reaching values  
442 of  $7.5 \pm 0.2$  at the end of the cycle. In period III (uncoupling B) the pH increased at  
443 the beginning of the cycle due to  $\text{NaHCO}_3$  supply, but it decreased during the famine  
444 phase ( Figure 2.e) (average of  $6.4 \pm 0.5$  at the end of the cycle). This reduction was a  
445 consequence of the microbial growth sustained by the intracellular carbon stored. In the  
446 respiration of the intracellular carbon,  $\text{CO}_2$  is released (Figure 1) acidifying the medium.  
447 In the coupled system, it was not observed a decrease of the pH since  $\text{NaHCO}_3$  was  
448 added immediately before the organic matter oxidation, which was mainly extracellular  
449 and took place during the feast phase.

450 Considering that respiration acidifies the medium and low pH environments constitute a  
451 competitive advantage for oleaginous microorganisms, it was explored the feasibility of  
452 selecting a culture with high TAG-storage capacity by the imposition of a double  
453 selective pressure in the SBR (period IV, days 254 – 307): N limitation during the feast  
454 phase and low pH during the famine. For nitrogen limitation, the same feeding strategy  
455 of period III was imposed (uncoupling type B). The pH was reduced by lowering the IC  
456 in the dilution water (Figure S3.b) to reduce the buffering capacity of the system and  
457 allow for greater acidification in the famine phase. The pH at the beginning of the cycle  
458 increased over 7.0 as a consequence of dilution water addition. However, during the  
459 feast phase, this parameter sharply decreased since the system buffering capacity was  
460 very low. For example, on day 287 of operation (Figure 2.f), the pH at the beginning of  
461 the cycle increased up to 7.6 but then decreased reaching a value of 3.8 at the end of the

462 cycle. On average, the pH at the end of the cycle decreased from  $6.5 \pm 0.4$  to  $4.0 \pm 0.3$   
463 between periods III and IV.

464 In period IV, the highest percentages of TAGs and the lowest of PHAs were observed at  
465 the end of the feast phase (Figure 3.a). For example, on day 287 of the enrichment  
466 cycle, a maximum of 30.6 wt % TAGs and 0.7 wt % PHAs were achieved, whereas at  
467 day 238 of the enrichment cycle (period III) only a 5.8 wt % TAG was accumulated.

468 These results showed that nitrogen limitation during the feast phase favoured the  
469 accumulation of storage compounds (advantage for accumulators), but low pH  
470 conditions during the famine only allowed for the survival of those species able to grow  
471 on the intracellular carbon source at low pH environments and resist these extreme  
472 conditions for a long time (TAG accumulators). The ratio between the length of the  
473 feast and the length of the cycle (feast/cycle ratio) was in period IV ( $0.12 \pm 0.03$ ) similar  
474 to the one measured in periods II and III ( $0.11 \pm 0.04$  and  $0.12 \pm 0.03$ , respectively) and  
475 also indicated an enrichment of the culture in microorganisms with high storage ability  
476 (Dionisi et al., 2005). Accumulation together with intracellular growth ( $0.24 \pm 0.06$ ),  
477 took longer than simultaneous accumulation and extracellular growth ( $0.21 \pm 0.07$ ,  
478 period I). The sum of accumulation and intracellular growth in periods II and III ( $0.35 \pm$   
479  $0.07$  and  $0.35 \pm 0.06$ , respectively) was higher than in period IV. This result suggested  
480 that the use of internal TAGs was easier than the use of internal PHAs for growth. In  
481 fact, VSS significantly increased, from  $0.50 \pm 0.16$  g/L and  $0.48 \pm 0.08$  g/L in periods II  
482 and III to  $0.94 \pm 0.13$  g/L in period IV.

### 483 **3.2.3 Evaluation of the system recovery capacity**

484 During period V (days 308 – 331) the selective pressure imposed by low pH during the  
485 famine phase was removed to test if it was possible to return to similar conditions to  
486 those of period III and recover the PHA-accumulation capacity of the system. For that

487 purpose, the IC of the dilution water was increased obtaining a pH of  $6.2 \pm 0.4$  at the  
488 end of the feast phase (similar to that of period III,  $6.5 \pm 0.4$ ). With it, the VSS  
489 concentration decreased, the feast/cycle ratio increased and the evolution of the different  
490 parameters monitored during the whole cycle (Figure 2.g) presented a similar trend to  
491 the observed in period III. From day 317 onwards an increasing PHA proportion in the  
492 storage compounds was observed (Figure 3.a), reaching a 21.6 wt % at the end of the  
493 feast phase on day 322 (Figure 2.g).

#### 494 **3.2.4 Statistic comparison of the SBR enrichment strategy**

495 The effect of imposing certain selective pressures in the enrichment SBR was  
496 statistically analysed to determine their impact over the preferent development of TAG  
497 or PHA producers, which correlated with the type of intracellular compounds  
498 accumulated. For that purpose, it was considered the composition of the intracellular  
499 compounds stored at the end of the feast phase in the SBR (operating at stationary state)  
500 during periods I – V.

501 Applying one-way ANOVA and Turkey post hoc tests (Table S1), it was observed  
502 statistically significant differences in the type of intracellular compounds accumulated  
503 when C and N feedings were uncoupled and N availability was limited to promote  
504 preferential PHA biosynthesis (same amount of C per unit of time) (periods I vs III).  
505 Besides, low pH imposition (period IV) maintaining the same conditions of those of  
506 period III, was also demonstrated to have a statistically significant impact over the  
507 preferent storage of TAGs.

508

509

510

511

### 512 **3.3 TAG and PHA accumulation**

#### 513 **3.3.1 Effect of the strategy of enrichment over the maximum storage capacity of** 514 **the enriched culture and the storage compounds composition**

515 In period I, the SBR was operated under excess of nitrogen and consequently, the  
516 effluent of the enrichment reactor used as inoculum in the FBR contained high nitrogen  
517 concentrations (up to 100 mg TN/L in the worst-case situations). In the accumulation  
518 assays performed on days 120 and 176 of operation (period I), the initial TN  
519 concentration was consumed during 9 – 10 hours due to biomass growth (Figure 4.a,  
520 4.b). Therefore, in period I, lipid accumulation was not the dominant process since the  
521 rate of accumulation was lower than the one of respiration (Papanikolaou and Aggelis,  
522 2010). The maximum accumulations of storage compounds measured were 21.7 wt %  
523 (19.7 wt % TAG, 2.0 wt % PHA) and 22.1 wt % (17.1 wt % TAG and 5 wt % PHA)  
524 reached on days 120 and 176, respectively. The maximum percentages of intracellular  
525 storage and production yields obtained in the FBR were not significantly different from  
526 those reached at the end of the feast phase in the SBR during period I (Figure 3.a). This  
527 was mainly related to the high N availability in the medium and the subsequent  
528 pathways used by the microorganisms to metabolize the substrate.

529 The maximum accumulation capacity of the MMC greatly increased after uncoupling C  
530 and N supply (periods II and III). Accumulations of 84.2 wt % (23 wt % TAGs and 61.2  
531 wt % PHAs) and 85.6 wt % (3.3 wt % TAGs and 82.3 wt % PHAs, respectively) were  
532 measured respectively on days 218 (type A) and 245 (type B) (Figure 3.b). The  
533 TAG:PHA ratio varied from 27:73 (day 218, type A) to 4:96 (day 245 type B), (Figure  
534 3.b; Table 3) showing that although intracellular storage was similar, type B  
535 configuration enhanced the enrichment of the culture in PHA accumulators. Lower  
536 biomass production yields, and higher  $Y_{PHA}$  and  $Y_{TAG}$  in comparison to those reached in

537 period I were obtained in the FBR assays performed during periods II and III (Table 3).  
538 Production yields were much lower in type A than in type B feeding strategy, which  
539 might be explained due to higher TAG and PHA accumulations measured at the  
540 beginning of the experiment.

541 An accumulation assay using the TAG-accumulating culture selected in the SBR during  
542 period IV (day 287) was carried. To possess comparable results and only evaluate the  
543 effect of low pH in the SBR over the maximum accumulation capacity, the pH in the  
544 FBR was increased by the addition of NaHCO<sub>3</sub> avoiding possible effects of low pH  
545 over accumulation (Figure 4.e). The highest percentage of intracellular TAG and TAG  
546 production yield (Figure 3.b; Table 3) were obtained in this assay. On day 287, it was  
547 accumulated 43.0 wt % TAGs and only 6.3 wt % PHAs implying a TAG:PHA ratio of  
548 87:13. Concomitant lactic acid production occurred with TAG accumulation at the end  
549 of the assay, 330 mg/L (equivalent to 11 Cmmol/L) of lactic acid were present in the  
550 reaction medium. This proved that the excess of carbon under oxygen and N limiting  
551 conditions pushed the microbial community to ferment the intracellularly accumulated  
552 TAGs to lactic acid.

553 Contrary, in the last accumulation assay performed on day 322 in period V (Figure 4.f),  
554 the capacity of PHA accumulation was recovered (Figure 3.b). The PHAs accumulated  
555 increased from 6.3 wt % (day 287, period IV) up to 34.8 wt %, and the ratio TAG:PHA  
556 varied from 87:13 to 11:88. Potentially, more operation cycles would increase the  
557 enrichment capacity until the levels achieved in period III (Table 3).

558 Therefore, the implementation of different selection strategies in the SBR allowed for  
559 the enrichment of the culture in microorganisms with a high TAG or PHA storage  
560 ability and promoted the subsequent preferential accumulation of one or another storage  
561 compound. In fact, the composition of the compounds stored at the end of the

562 accumulation assays was proportional to that of the enrichment reactor at the end of the  
563 feast phase when comparing the same operational periods (Figure 3, Table 2, Table 3).  
564 No statistically significant differences were observed between both pair of data (t-test  
565 for independent samples,  $t(5) = 0.331$ ,  $p = 0.749$  (see details in Table S1)). Operating  
566 the SBR with type B uncoupling strategy, N limitation during the feast phase and pH  
567  $6.4 \pm 0.4$  at the end of the cycle was proven the best strategy to obtain intracellular  
568 compounds rich on PHAs (85.6 wt % PHAs,  $Y_{\text{PHA}} = 0.80$ , and TAG:PHA = 4:96 ). The  
569 same operational conditions were proven optimal to maximise TAG accumulation but  
570 maintaining the pH low during the famine phase ( $4.0 \pm 0.3$ ) to select for TAG  
571 accumulators (43.0 wt % TAGs,  $Y_{\text{TAG}} = 0.67$ , and TAG:PHA = 87:13) (Figure S5)

### 572 **3.3.2 Comparison with literature**

573 After reviewing available literature concerning the microbial valorization of lipidic  
574 feedstocks for TAG or PHAs production (information summarised in Table 4), it was  
575 observed that most of the research works performed to date were focused on the use of  
576 pure cultures and vegetable oils as a substrate. Very few studies considered the use of  
577 animal fats (Herrero et al., 2018; Lopes et al., 2018; Riedel et al., 2015; Sangkharak et  
578 al., 2020; Van Thuoc et al., 2019), specifically, only Van Thuoc et al. (2019) and  
579 Sangkharak et al. (2020) explored the production of PHAs from feedstocks rich in fish  
580 lipids. Overall, these works showed that the use of animal fats, which are complex  
581 lipidic substrates, compromised the productivity of the system.

582 The maximum quantity of TAGs accumulated in this study (period IV), was comparable  
583 or even higher than the one obtained in previous experiments using both pure (Chan et  
584 al., 2018; Lopes et al., 2018) and mixed cultures (Tamis et al., 2015) (Table 4).  
585 Regarding PHA production, the results reached during period III (82.3 %wt PHAs,  
586  $Y_{\text{PHA/S}} = 0.80$  Cmmol/Cmmol) were very similar to those obtained when using soybean

587 oil for PHA biosynthesis by a pure culture (*Cupriavidus necator* 81 %wt of PHA,  $Y_{\text{PHA}}$   
588 0.85 g/g (da Cruz Pradella et al., 2012)) (Table 4).

589 None of the experiments presented in Table 4 showed the possibility of storing TAGs or  
590 PHAs in the same system. However, their simultaneous accumulation has been proven  
591 with other non-lipidic substrates: Hori et al. (2009) investigated the simultaneous  
592 production of TAGs and PHAs by *Rhodococcus aetherivorans* (Hori et al., 2009);  
593 Castro et al. (2018) obtained 33 wt % of neutral lipids containing 77 % TAG and 4 wt  
594 % of PHA in a previous enriched culture using lubricant-based wastewater (Castro et  
595 al., 2018); and Fra-Vázquez et al. (2018) obtained 46 wt % TAG and 7.4 wt % PHA in a  
596 MMC when using crude glycerol as a substrate (Fra-Vázquez et al., 2018).

### 597 **3.3.3 Opportunities of the process: TAG vs PHA production**

598 The present research demonstrated that it was possible to drive microbial metabolism  
599 towards the preferential production of two different storage materials in the same  
600 system using a unique feedstock: TAGs mainly formed by oleic and linoleic acids, and  
601 PHAs composed of hydroxybutyrate units.

602 TAG accumulation via *ex novo* pathway from waste fish oil did not lead to the  
603 transformation of the storage lipids into upgraded fatty acid profiles (Carsanba et al.,  
604 2018). Intracellular TAGs presented a composition proportional to that of the substrate  
605 (Table 1) and the lack of specificity is expected to hinder their use in industries such as  
606 pharmaceutical, cosmetic, or food-processing. However, the mixture of FFA obtained  
607 appeared suitable for biodiesel production (Bušić et al., 2018; Sawangkeaw and  
608 Ngamprasertsith, 2013). Therefore, it should be evaluated if the recovery of microbial  
609 TAGs would be more sustainable and economically favourable than the waste fish oil  
610 pretreatment needed before transesterification (Sawangkeaw and Ngamprasertsith,  
611 2013).

612 On the other hand, polyhydroxybutyrate (PHB) biopolymers are a valuable feedstock  
613 for bioplastics production due to their material properties, similar to those of  
614 polypropylene (Sudesh et al., 2000), and appear as a higher way of valorization than  
615 energy production from TAGs (Wallace et al., 2017). PHB obtention using MMCs,  
616 saving an operation unit, and considering a waste stream as a substrate, would strongly  
617 reduce production costs, the major restriction for wide PHA commercialization and  
618 industrialization (Surendran et al., 2020).

619

#### 620 **4. CONCLUSIONS**

621 This process demonstrated versatility and efficiency in non-pre-fermented residual fish-  
622 canning oil valorization into TAGs and PHAs using a MMC. The implementation of  
623 different selection strategies for the enrichment of the culture in microbial species with  
624 high TAG or PHA storage ability had a significant impact on the selection of the  
625 dominant metabolic pathways in the system, which allowed to increase and control the  
626 quantity and type of compounds accumulated. When carbon and nitrogen were fed  
627 separately and the amount of nitrogen added was limited, PHA accumulation and  
628 productivity substantially increased compared to that obtained in the coupled system  
629 (from 5.0 wt % to 82.3 wt % and from 0.03 Cmmol<sub>PHA</sub>/Cmmols to 0.80  
630 Cmmol<sub>PHA</sub>/Cmmols) whereas TAG production was insignificant (TAG:PHA ratio of  
631 4:96). Furthermore, when low pH conditions in the famine were considered as an  
632 additional selective pressure in the uncoupled system, TAG accumulation dominated  
633 and it was possible to reach a maximum 43.0 wt % TAG in the FBR (TAG:PHA ratio of  
634 87:13) obtaining a production yield of 0.67 Cmmol<sub>TAG</sub>/Cmmols.

635

636 **5. ACKNOWLEDGEMENTS**

637 This research was supported by the Spanish Government (AEI) through the  
638 TREASURE project [CTQ2017-83225-C2-1-R]. Lucía Argiz is a Xunta de Galicia  
639 fellow (2019), [ED 481A-2019/083], grant co-funded by the operative program FSE  
640 Galicia 2014-2020. Lucía Argiz, Ángeles Val del Río, and Anuska Mosquera-Corral  
641 belong to the Galician Competitive Research Group GRC ED431C 2017/29. All these  
642 programs are co-funded by the FEDER (EU).

643

644 **6. REFERENCES**

645 Ahmad, T., Belwal, T., Li, L., Ramola, S., Aadil, R.M., Abdullah, Xu, Y., Zisheng, L.,  
646 2020. Utilization of wastewater from edible oil industry, turning waste into  
647 valuable products: A review. *Trends Food Sci. Technol.* 99, 21–33.  
648 <https://doi.org/10.1016/j.tifs.2020.02.017>

649 Alvarez, H.M., Steinbüchel, A., 2003. Triacylglycerols in prokaryotic microorganisms.  
650 *Appl. Microbiol. Biotechnol.* 60, 367–376. [https://doi.org/10.1007/s00253-002-](https://doi.org/10.1007/s00253-002-1135-0)  
651 1135-0

652 APHA/AWWA/WEF, 2017. *Standard Methods for the Examination of Water and*  
653 *Wastewater*, 23rd ed., American Public Health Association, Washington, DC, USA.  
654 *Am. Public Heal. Assoc. Washington, DC, USA.* [https://doi.org/ISBN](https://doi.org/ISBN9780875532356)  
655 9780875532356

656 Basnett, P., Marcello, E., Lukasiewicz, B., Panchal, B., Nigmatullin, R., Knowles, J.C.,  
657 Roy, I., 2018. Biosynthesis and characterization of a novel, biocompatible medium  
658 chain length polyhydroxyalkanoate by *Pseudomonas mendocina* CH50 using  
659 coconut oil as the carbon source. *J. Mater. Sci. Mater. Med.* 29.

660 <https://doi.org/10.1007/s10856-018-6183-9>

661 Becker, P., 2010. Understanding and Optimizing the Microbial Degradation of Olive  
662 Oil: A Case Study with the Thermophilic Bacterium *Geobacillus thermoleovorans*  
663 IHI-91, Olives and Olive Oil in Health and Disease Prevention. Elsevier Inc.  
664 <https://doi.org/10.1016/B978-0-12-374420-3.00042-5>

665 Bušić, A., Kundas, S., Morzak, G., Belskaya, H., Mardetko, N., Šantek, M.I., Komes,  
666 D., Novak, S., Šantek, B., 2018. Recent trends in biodiesel and biogas production.  
667 *Food Technol. Biotechnol.* 56, 152–173.  
668 <https://doi.org/10.17113/ftb.56.02.18.5547>

669 Campanari, S., E Silva, F.A., Bertin, L., Villano, M., Majone, M., 2014. Effect of the  
670 organic loading rate on the production of polyhydroxyalkanoates in a multi-stage  
671 process aimed at the valorization of olive oil mill wastewater. *Int. J. Biol.*  
672 *Macromol.* 71, 34–41. <https://doi.org/10.1016/j.ijbiomac.2014.06.006>

673 Carsanba, E., Papanikolaou, S., Erten, H., 2018. Production of oils and fats by  
674 oleaginous microorganisms with an emphasis given to the potential of the  
675 nonconventional yeast *Yarrowia lipolytica*. *Crit. Rev. Biotechnol.* 38, 1230–1243.  
676 <https://doi.org/10.1080/07388551.2018.1472065>

677 Castro, A.R., Silva, P.T.S., Castro, P.J.G., Alves, E., Domingues, M.R.M., Pereira,  
678 M.A., 2018. Tuning culturing conditions towards the production of neutral lipids  
679 from lubricant-based wastewater in open mixed bacterial communities. *Water Res.*  
680 144, 532–542. <https://doi.org/10.1016/j.watres.2018.07.068>

681 Chan, L.G., Cohen, J.L., Ozturk, G., Hennebelle, M., Taha, A.Y., De Moura Bell,  
682 J.M.L.N., 2018. Bioconversion of cheese whey permeate into fungal oil by *Mucor*  
683 *circinelloides*. *J. Biol. Eng.* 12, 1–14. <https://doi.org/10.1186/s13036-018-0116-5>

684 Chipasa, K.B., Mędrzycka, K., 2006. Behavior of lipids in biological wastewater  
685 treatment processes. *J. Ind. Microbiol. Biotechnol.* 33, 635–645.  
686 <https://doi.org/10.1007/s10295-006-0099-y>

687 Cristóvão, R.O., Botelho, C.M., Martins, R.J.E., Loureiro, J.M., Boaventura, R.A.R.,  
688 2015. Fish canning industry wastewater treatment for water reuse - A case Study.  
689 *J. Clean. Prod.* 87, 603–612. <https://doi.org/10.1016/j.jclepro.2014.10.076>

690 da Cruz Pradella, J.G., Ienczak, J.L., Delgado, C.R., Taciro, M.K., 2012. Carbon source  
691 pulsed feeding to attain high yield and high productivity in poly(3-  
692 hydroxybutyrate) (PHB) production from soybean oil using *Cupriavidus necator*.  
693 *Biotechnol. Lett.* 34, 1003–1007. <https://doi.org/10.1007/s10529-012-0863-1>

694 Dionisi, D., Majone, M., Vallini, G., Gregorio, S. Di, Beccari, M., 2005. Effect of the  
695 Applied Organic Load Rate on Biodegradable Polymer Production by Mixed  
696 Microbial Cultures in a Sequencing Batch Reactor.  
697 <https://doi.org/10.1002/bit.20683>

698 Donot, F., Fontana, A., Baccou, J.C., Strub, C., Schorr-Galindo, S., 2014. Single cell  
699 oils (SCOs) from oleaginous yeasts and moulds: Production and genetics. *Biomass*  
700 *and Bioenergy* 68, 135–150. <https://doi.org/10.1016/j.biombioe.2014.06.016>

701 Fra-Vázquez, A., Pedrouso, A., Palmeiro-Sánchez, T., Moralejo-Gárate, H., Mosquera-  
702 Corral, A., 2018. Feasible microbial accumulation of triacylglycerides from crude  
703 glycerol. *J. Chem. Technol. Biotechnol.* 93, 2644–2651.  
704 <https://doi.org/10.1002/jctb.5618>

705 Garay, L.A., Boundy-Mills, K.L., German, J.B., 2014. Accumulation of high-value  
706 lipids in single-cell microorganisms: A mechanistic approach and future  
707 perspectives. *J. Agric. Food Chem.* 62, 2709–2727.

708 <https://doi.org/10.1021/jf4042134>

709 Gujjala, L.K.S., Kumar, S.P.J., Talukdar, B., Dash, A., Kumar, S., Sherpa, K.C.,  
710 Banerjee, R., 2019. Biodiesel from oleaginous microbes: opportunities and  
711 challenges. *Biofuels* 10, 45–59. <https://doi.org/10.1080/17597269.2017.1402587>

712 Herrero, O.M., Villalba, M.S., Lanfranconi, M.P., Alvarez, H.M., 2018. *Rhodococcus*  
713 bacteria as a promising source of oils from olive mill wastes. *World J. Microbiol.*  
714 *Biotechnol.* 34, 0. <https://doi.org/10.1007/s11274-018-2499-3>

715 Hori, K., Abe, M., Unno, H., 2009. Production of triacylglycerol and poly(3-  
716 hydroxybutyrate-co-3-hydroxyvalerate) by the toluene-degrading bacterium  
717 *Rhodococcus aetherivorans* IAR1. *J. Biosci. Bioeng.* 108, 319–324.  
718 <https://doi.org/10.1016/j.jbiosc.2009.04.020>

719 Huang, C., Luo, M.T., Chen, X.F., Qi, G.X., Xiong, L., Lin, X.Q., Wang, C., Li, H.L.,  
720 Chen, X. De, 2017. Combined “de novo” and “ex novo” lipid fermentation in a  
721 mix-medium of corncob acid hydrolysate and soybean oil by *Trichosporon*  
722 *dermatis*. *Biotechnol. Biofuels* 10, 1–11. [https://doi.org/10.1186/s13068-017-0835-](https://doi.org/10.1186/s13068-017-0835-8)  
723 8

724 Jimenez-diaz, L., Caballero, A., Segura, A., 2019. Aerobic Utilization of Hydrocarbons,  
725 Oils, and Lipids. *Aerob. Util. Hydrocarb. Oils, Lipids* 291–313.  
726 <https://doi.org/10.1007/978-3-319-50418-6>

727 Kourmentza, C., Plácido, J., Venetsaneas, N., Burniol-Figols, A., Varrone, C., Gavala,  
728 H.N., Reis, M.A.M., 2017. Recent Advances and Challenges towards Sustainable  
729 Polyhydroxyalkanoate (PHA) Production. *Bioengineering* 4, 55.  
730 <https://doi.org/10.3390/bioengineering4020055>

731 Kosseva M., Webb C., 2013. Food industry wastes. Assessment and Recuperation of

732 Commodities, 1st ed, Academic press.

733 Kumar, M., Ghosh, P., Khosla, K., Thakur, I.S., 2018. Recovery of  
734 polyhydroxyalkanoates from municipal secondary wastewater sludge. *Bioresour.*  
735 *Technol.* 255, 111–115. <https://doi.org/10.1016/j.biortech.2018.01.031>

736 Kumar, M., Rathour, R., Singh, R., Sun, Y., Pandey, A., Gnansounou, E., Andrew Lin,  
737 K.Y., Tsang, D.C.W., Thakur, I.S., 2020. Bacterial polyhydroxyalkanoates:  
738 Opportunities, challenges, and prospects. *J. Clean. Prod.* 263, 121500.  
739 <https://doi.org/10.1016/j.jclepro.2020.121500>

740 Leng, L., Zhang, W., Peng, H., Li, H., Jiang, S., Huang, H., 2020. Nitrogen in bio-oil  
741 produced from hydrothermal liquefaction of biomass: A review. *Chem. Eng. J.*  
742 401, 126030. <https://doi.org/10.1016/j.cej.2020.126030>

743 Lopes, M., Gomes, A.S., Silva, C.M., Belo, I., 2018. Microbial lipids and added value  
744 metabolites production by *Yarrowia lipolytica* from pork lard. *J. Biotechnol.* 265,  
745 76–85. <https://doi.org/10.1016/j.jbiotec.2017.11.007>

746 Lorini, L., di Re, F., Majone, M., Valentino, F., 2020. High rate selection of PHA  
747 accumulating mixed cultures in sequencing batch reactors with uncoupled carbon  
748 and nitrogen feeding. *N. Biotechnol.* 56, 140–148.  
749 <https://doi.org/10.1016/j.nbt.2020.01.006>

750 Maqbool, A., Strandvik, B., Stallings, V.A., 2011. The skinny on tuna fat: Health  
751 implications. *Public Health Nutr.* 14, 2049–2054.  
752 <https://doi.org/10.1017/S1368980010003757>

753 Md Din, M.F., Ujang, Z., van Loosdrecht, M.C.M., Ahmad, A., Sairan, M.F.,  
754 2006. Optimization of nitrogen and phosphorus limitation for better biodegradable  
755 plastic production and organic removal using single fed-batch mixed cultures

756 andrenewable resources. *Water Sci. Technol.* 53, 15–  
757 20. <https://doi.org/10.2166/wst.2006.164>Oliveira, C.S.S., Silva, C.E., Carvalho,  
758 G., *Biotechnol.* 37, 69–79

759 Oliveira, C.S.S., Silva, C.E., Carvalho, G., Reis, M.A., 2017. Strategies for efficiently  
760 selecting PHA producing mixed microbial cultures using complex feedstocks:  
761 Feast and famine regime and uncoupled carbon and nitrogen availabilities. *N.*  
762 *Biotechnol.* 37, 69–79. <https://doi.org/10.1016/j.nbt.2016.10.008>

763 Papanikolaou, S., Aggelis, G., 2010. *Yarrowia lipolytica*: A model microorganism used  
764 for the production of tailor-made lipids. *Eur. J. Lipid Sci. Technol.* 112, 639–654.  
765 <https://doi.org/10.1002/ejlt.200900197>

766 Patel, A., Matsakas, L., 2019. A comparative study on de novo and ex novo lipid  
767 fermentation by oleaginous yeast using glucose and sonicated waste cooking oil.  
768 *Ultrason. Sonochem.* 52, 364–374. <https://doi.org/10.1016/j.ultsonch.2018.12.010>

769 Pérez-Arauz, A.O., Aguilar-Rabiela, A.E., Vargas-Torres, A., Rodríguez-Hernández,  
770 A.I., Chavarría-Hernández, N., Vergara-Porras, B., López-Cuellar, M.R., 2019.  
771 Production and characterization of biodegradable films of a novel  
772 polyhydroxyalkanoate (PHA) synthesized from peanut oil. *Food Packag. Shelf Life*  
773 20, 100297. <https://doi.org/10.1016/j.fpsl.2019.01.001>

774 Revellame, E.D., Hernandez, R., French, W., Holmes, W.E., Benson, T.J., Pham, P.J.,  
775 Forks, A., Callahan, R., 2012. Lipid storage compounds in raw activated sludge  
776 microorganisms for biofuels and oleochemicals production. *RSC Adv.* 2, 2015–  
777 2031. <https://doi.org/10.1039/c2ra01078j>

778 Riedel, S.L., Jahns, S., Koenig, S., Bock, M.C.E., Brigham, C.J., Bader, J., Stahl, U.,  
779 2015. Polyhydroxyalkanoates production with *Ralstonia eutropha* from low quality

780 waste animal fats. *J. Biotechnol.* 214, 119–127.  
781 <https://doi.org/10.1016/j.jbiotec.2015.09.002>

782 Sabapathy, P.C., Devaraj, S., Meixner, K., Anburajan, P., Kathirvel, P., Ravikumar, Y.,  
783 Zabed, H.M., Qi, X., 2020. Recent developments in Polyhydroxyalkanoates  
784 (PHAs) production – A review. *Bioresour. Technol.* 123132.  
785 <https://doi.org/10.1016/j.biortech.2020.123132>

786 Sangkharak, K., Paichid, N., Yunu, T., Klomklao, S., Prasertsan, P., 2020. Utilisation of  
787 tuna condensate waste from the canning industry as a novel substrate for  
788 polyhydroxyalkanoate production. *Biomass Convers. Biorefinery.*  
789 <https://doi.org/10.1007/s13399-019-00581-4>

790 Santamauro, F., Whiffin, F.M., Scott, R.J., Chuck, C.J., 2014. Low-cost lipid production  
791 by an oleaginous yeast cultured in non-sterile conditions using model waste  
792 resources. *Biotechnol. Biofuels* 7, 1–11. <https://doi.org/10.1186/1754-6834-7-34>

793 Sawangkeaw, R., Ngamprasertsith, S., 2013. A review of lipid-based biomasses as  
794 feedstocks for biofuels production. *Renew. Sustain. Energy Rev.* 25, 97–108.  
795 <https://doi.org/10.1016/j.rser.2013.04.007>

796 Silva, F., Campanari, S., Matteo, S., Valentino, F., Majone, M., Villano, M., 2017.  
797 Impact of nitrogen feeding regulation on polyhydroxyalkanoates production by  
798 mixed microbial cultures. *N. Biotechnol.* 37, 90–98.  
799 <https://doi.org/10.1016/j.nbt.2016.07.013>

800 Song, J.H., Jeon, C.O., Choi, M.H., Yoon, S.C., Park, W., 2008. Polyhydroxyalkanoate  
801 (PHA) production using waste vegetable oil by *Pseudomonas* sp. strain DR2.  
802 *J. Microbiol. Biotechnol.* 18, 1408–1415.

803 Sudesh, K., Abe, H., Doi, Y., 2000. Synthesis, structure and properties of

804 polyhydroxyalkanoates: Biological polyesters. *Prog. Polym. Sci.* 25, 1503–1555.  
805 [https://doi.org/10.1016/S0079-6700\(00\)00035-6](https://doi.org/10.1016/S0079-6700(00)00035-6)

806 Surendran, A., Lakshmanan, M., Chee, J.Y., Sulaiman, A.M., Thuoc, D. Van, Sudesh,  
807 K., 2020. Can Polyhydroxyalkanoates Be Produced Efficiently From Waste Plant  
808 and Animal Oils? *Front. Bioeng. Biotechnol.* 8.  
809 <https://doi.org/10.3389/fbioe.2020.00169>

810 Tamis, J., Sorokin, D.Y., Jiang, Y., Van Loosdrecht, M.C.M., Kleerebezem, R., 2015.  
811 Lipid recovery from a vegetable oil emulsion using microbial enrichment cultures.  
812 *Biotechnol. Biofuels* 8, 1–11. <https://doi.org/10.1186/s13068-015-0228-9>

813 Tan, G.Y.A., Chen, C.L., Li, L., Ge, L., Wang, L., Razaad, I.M.N., Li, Y., Zhao, L.,  
814 Mo, Y., Wang, J.Y., 2014. Start a research on biopolymer polyhydroxyalkanoate  
815 (PHA): A review. *Polymers (Basel)*. 6, 706–754.  
816 <https://doi.org/10.3390/polym6030706>

817 Van Thuoc, D., My, D.N., Loan, T.T., Sudesh, K., 2019. Utilization of waste fish oil  
818 and glycerol as carbon sources for polyhydroxyalkanoate production by  
819 *Salinivibrio* sp. M318. *Int. J. Biol. Macromol.* 141, 885–892.  
820 <https://doi.org/10.1016/j.ijbiomac.2019.09.063>

821 Vasiliadou, I.A., Bellou, S., Daskalaki, A., Tomaszewska-Hetman, L., Chatzikotoula,  
822 C., Kompoti, B., Papanikolaou, S., Vayenas, D., Pavlou, S., Aggelis, G., 2018.  
823 Biomodification of fats and oils and scenarios of adding value on renewable fatty  
824 materials through microbial fermentations: Modelling and trials with *Yarrowia*  
825 *lipolytica*. *J. Clean. Prod.* 200, 1111–1129.  
826 <https://doi.org/10.1016/j.jclepro.2018.07.187>

827 Vishniac, W., Santer, M., 1957. The *thiobacilli*. *Bacteriol. Rev.* 21, 195–213.

828 Wakelin, N.G., Forster, C.F., 1997. An investigation into microbial removal of fats, oils  
829 and greases. *Bioresour. Technol.* 59, 37–43. [https://doi.org/10.1016/S0960-](https://doi.org/10.1016/S0960-8524(96)00134-4)  
830 [8524\(96\)00134-4](https://doi.org/10.1016/S0960-8524(96)00134-4)

831 Wallace, T., Gibbons, D., O’Dwyer, M., Curran, T.P., 2017. International evolution of  
832 fat, oil and grease (FOG) waste management – A review. *J. Environ. Manage.* 187,  
833 424–435. <https://doi.org/10.1016/j.jenvman.2016.11.003>

834 Waller, J.L., Green, P.G., Loge, F.J., 2012. Mixed-culture polyhydroxyalkanoate  
835 production from olive oil mill pomace. *Bioresour. Technol.* 120, 285–289.  
836 <https://doi.org/10.1016/j.biortech.2012.06.024>

837 Wu, H., Gao, X., Wu, M., Zhu, Y., Xiong, R., Ye, S., 2020. The efficiency and risk to  
838 groundwater of constructed wetland system for domestic sewage treatment - a case  
839 study in Xiantao, China. *J. Clean. Prod.* 123384.  
840 <https://doi.org/10.1016/j.jclepro.2020.123384>

841 Yadav, B., Pandey, A., Kumar, L.R., Tyagi, R.D., 2020. Bioconversion of waste  
842 (water)/residues to bioplastics- A circular bioeconomy approach. *Bioresour.*  
843 *Technol.* 298, 122584. <https://doi.org/10.1016/j.biortech.2019.122584>

844

**Figure 1.** Simplified metabolic pathways describing TAG and PHA production from lipids in microbial cultures. Free fatty acids (FFA) yielded after the substrate hydrolysis can be catabolized (direct respiration) or accumulated as reserve materials (TAGs or PHAs produced by the *ex novo* or PHA biosynthesis pathways, respectively).

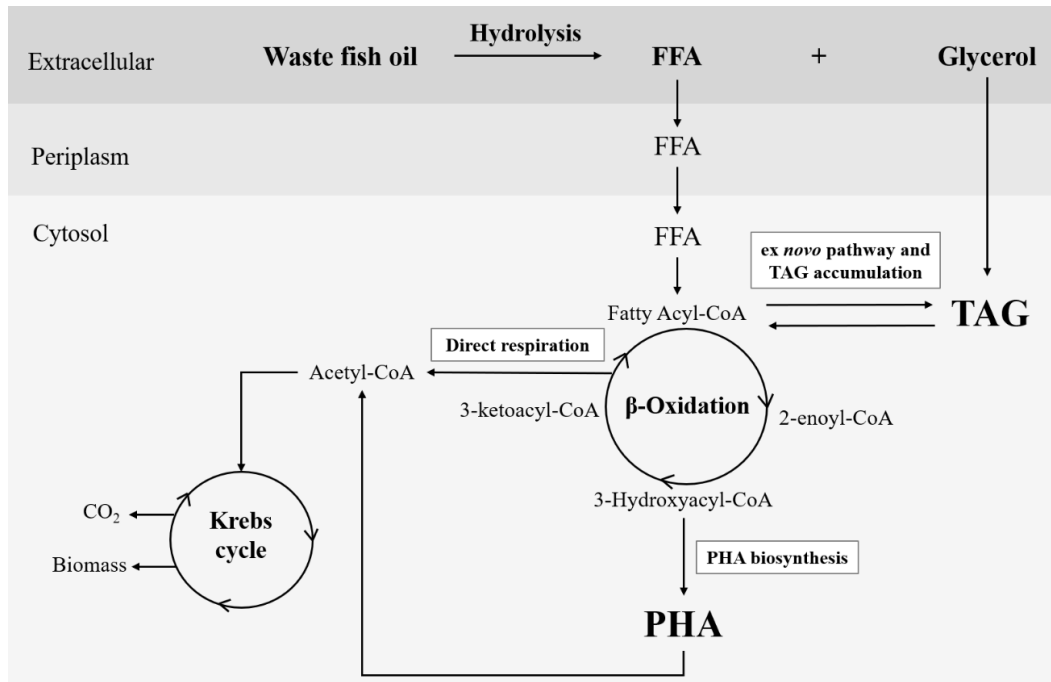


**Figure 2.** Characterization of the SBR enrichment cycles. Concentrations of DO (—), X (---), pH (●), TN (◆), TAG + PHA (○).

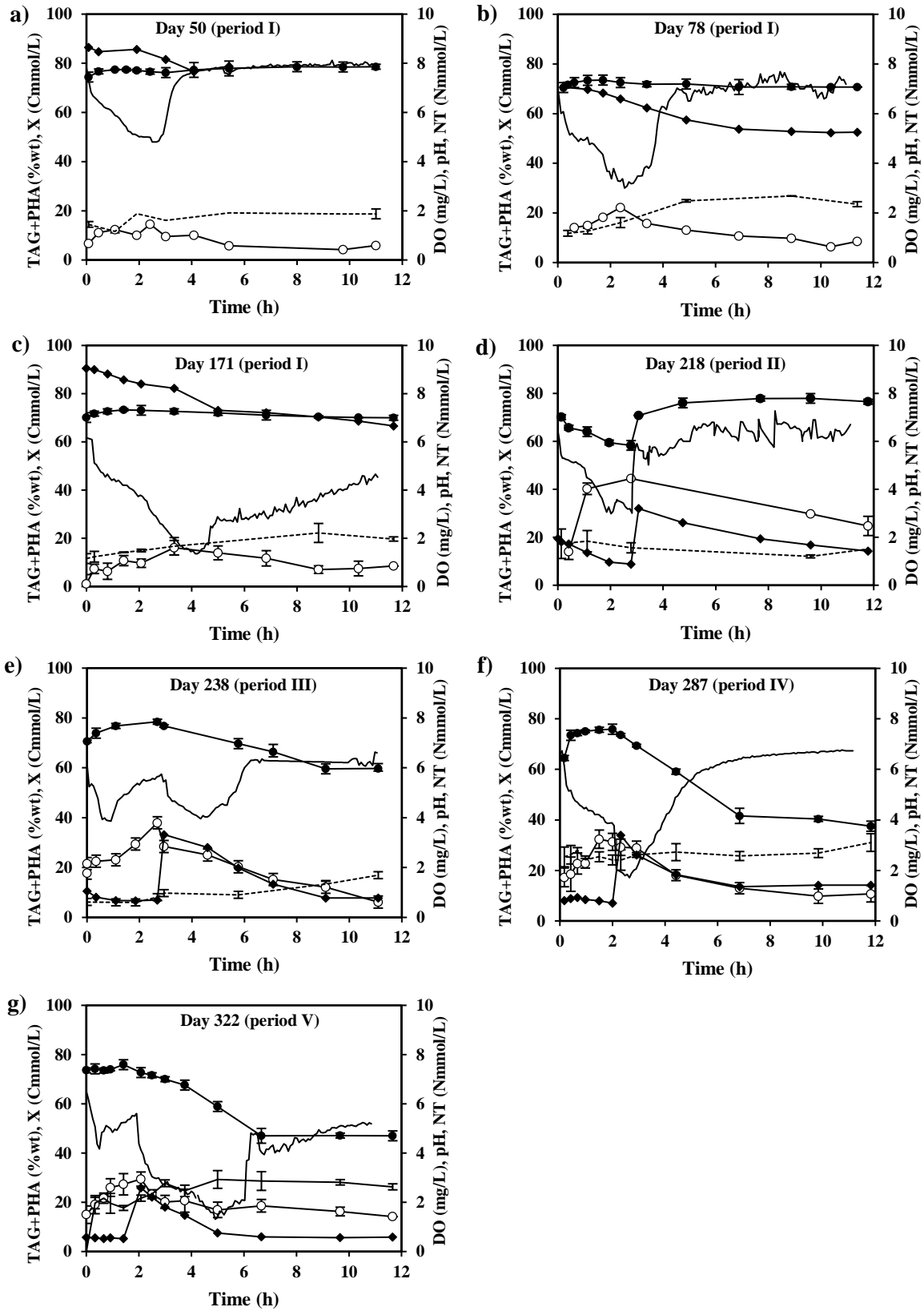


**Figure3.** Maximum intracellular storage and composition: a) at the end of the feast phase in the SBR; b) at the end of the accumulation assays in the FBR. Percentages of intracellular TAGs ( $\Delta$ ), and PHAs ( $\times$ ) in the biomass. Composition expressed in percentages of palmitic ( $\square$ ), stearic ( $\blacksquare$ ), oleic ( $\square$ ), linoleic ( $\blacksquare$ ) and PHB ( $\boxtimes$ ).

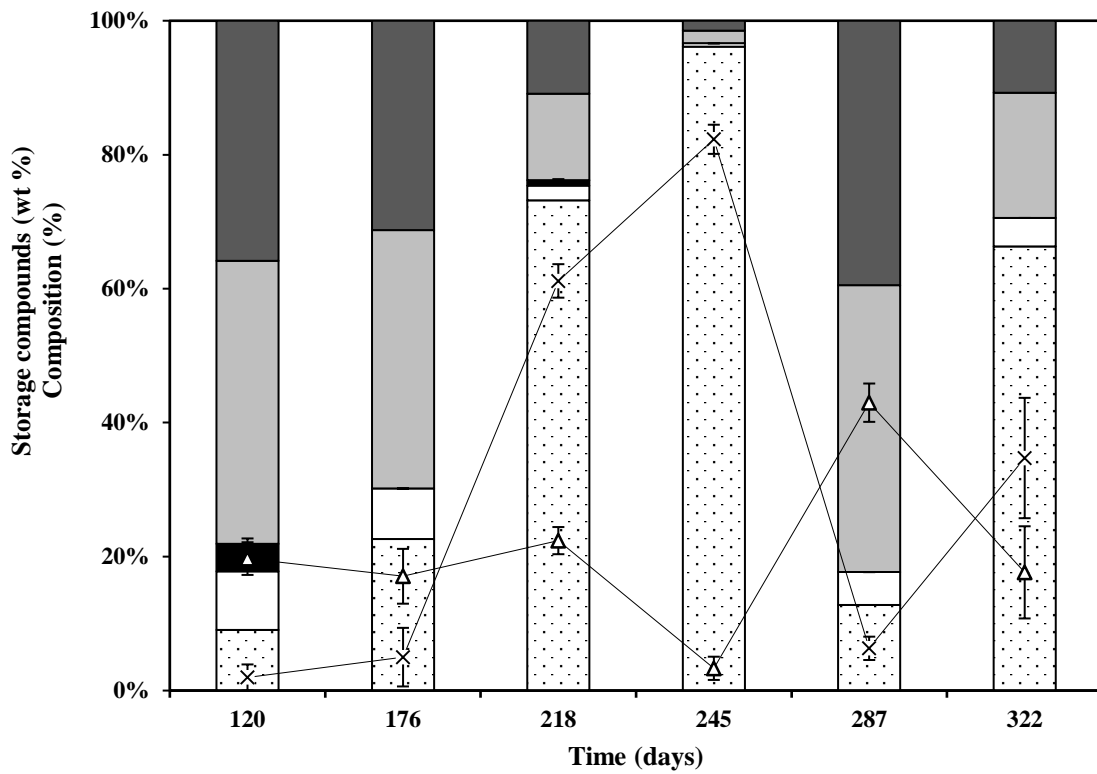
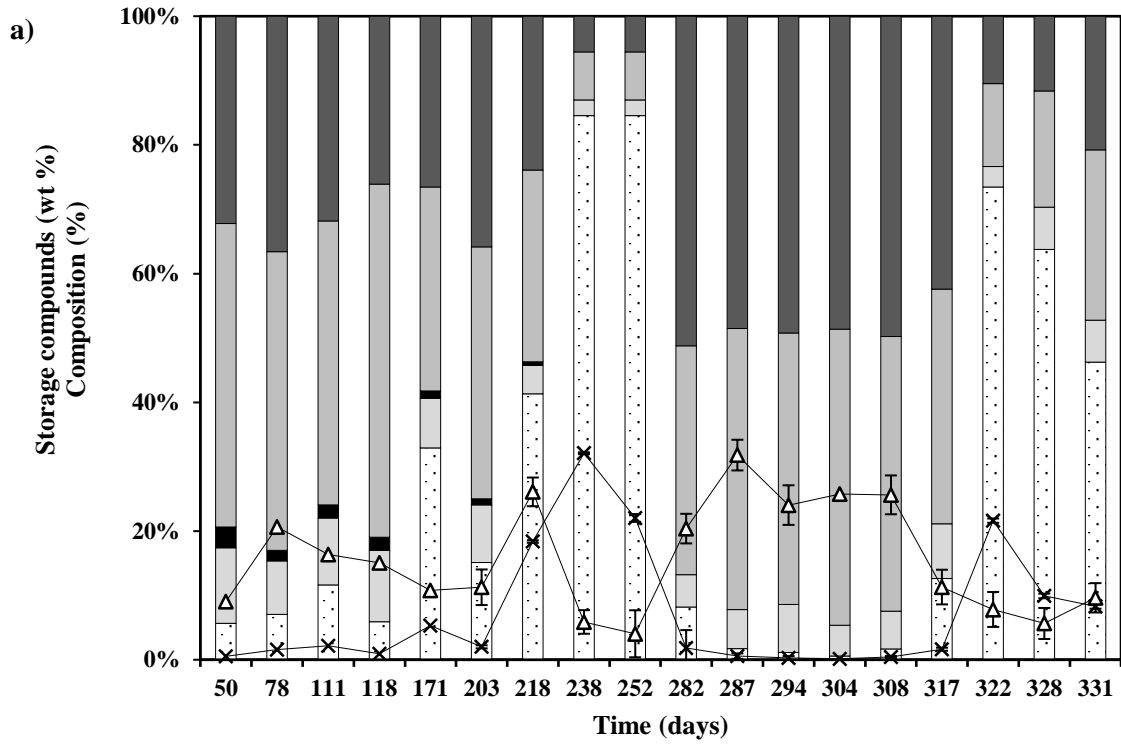


**Figure 4.** Complete characterization of the accumulation assays performed in the FBR. X (---), pH (●), TN (◆), TAGs (Δ), PHAs (×), oil (■).

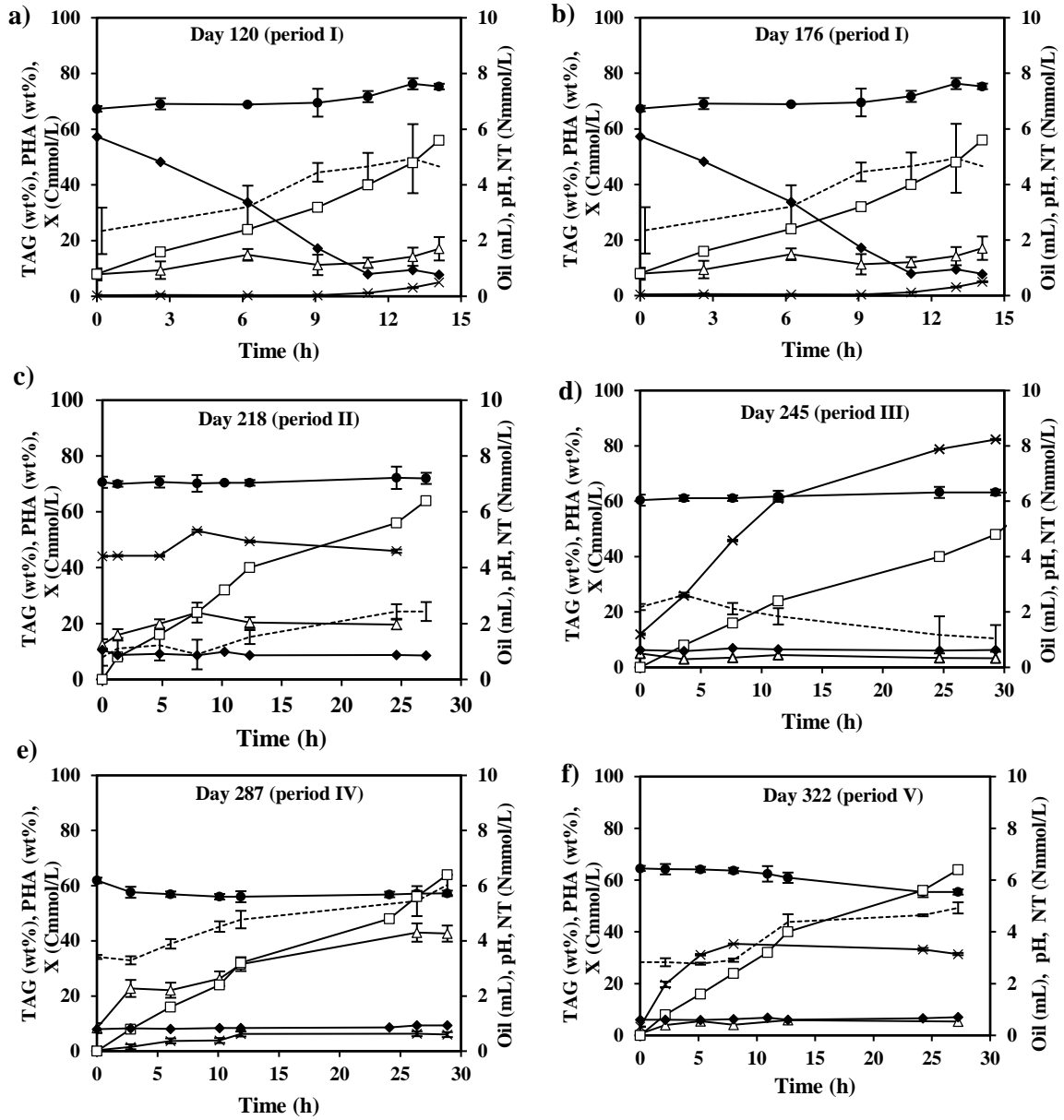


**Table 1.** Characteristics of the fish-canning industry oil used as a substrate.

Parameter	Value
pH	3.75 ± 0.20
Conductivity (μS/cm)	0.60 ± 0.10
Density (g/L)	900 ± 10
TS (g/g)	0.853 ± 0.018
VS (g/g)	0.852 ± 0.019
VS/TS (%)	99.89
COD (g/g)	2.50 ± 0.11
Lipids (g/g)	0.823 ± 0.089
Composition (wt%)	Palmitic acid: 10.3 ± 0.4
	Stearic acid: 2.5 ± 1.0
	Oleic acid: 38.3 ± 1.6
	Linoleic acid: 31.2 ± 1.5
	Others: 17.7 ± 4.2

**Table 2.** Intracellular storage, kinetic parameters and yields determined in different cycles monitored in the enrichment SBR.

Operational period	I	I	I	II	III	IV	V
Day of operation	Day 50	Day 78	Day 171	Day 218	Day 238	Day 287	Day 322
<b>% wt max.</b>							
TAGs	13.7	20.6	10.8	25.8	5.8	30.6	7.8
PHAs	0.9	1.6	5.3	18.4	32.1	0.7	21.6
<b>Composition</b>							
TAG:PHA	94:6	93:7	67:33	42:58	15:85	98:2	27:73
Palmitic:Stearic:Oleic:Linoleic	14:4:44:33	9:2:50:39	11:2:47:40	8:0:51:41	16:0:48:36	6:0:47:47:	12:0:49:40
PHB:PHV	100:0	100:0	100:0	100:0	100:0	100:0	100:0
<b>q (Cmmol/Cmmol·h)</b>							
$q_{TAG/X-h}$	0.018	0.089	0.034	0.030	0.000	0.131	0.000
$q_{PHA/X-h}$	0.001	0.005	0.024	0.065	0.069	0.001	0.048
$-q_{N/X-h}^{(1)}$	0.053 – 0.022	0.196 – 0.029	0.079 – 0.031	0.002 – 0.000	0.005 – 0.003	0.000 – 0.002	0.000 – 0.005
$q_{X/S-h}^{(1)}$	0.002 – 0.000	0.002 – 0.012	0.005 – 0.015	0.019 – 0.017	0.000 – 0.027	0.000 – 0.017	0.000 – 0.017
<b>Y (Cmmol/Cmmol)</b>							
$Y_{TAG/S}$	0.053	0.098	0.127	0.168	0.000	0.467	0.000
$Y_{PHA/S}$	0.002	0.006	0.041	0.078	0.115	0.001	0.147
$Y_{X/S}^{(1)}$	0.035 – 0.000	0.035 – 0.310	0.075 – 0.112	0.052 – 0.224	0.000 – 0.289	0.000 – 0.171	0.000 – 0.449

<sup>(1)</sup> Data regarding feast (left) and famine (right) phases: feast – famine.

**Table 3.** Intracellular storage, kinetic parameters and yields determined in the batch assays performed in the accumulation FBR.

<b>Operational period</b>	<b>I</b>	<b>I</b>	<b>II</b>	<b>III</b>	<b>IV</b>	<b>V</b>
<b>Day of operation</b>	120	176	218	245	287	322
<b>% wt max.</b>						
TAGs	19.7	17.1	23.0	3.3	43.0	17.6
PHAs	2.0	5.0	61.2	82.3	6.3	34.8
<b>Composition</b>						
TAG:PHA	91:9	77:23	27:73	4:96	87:13	34:66
Palmitic:Stearic:Oleic:Linoleic	10:5:46:39	10:0:50:40	8:3:46:43	12:0:48:39	6:0:49:45	13:0:56:32
PHB:PHV	100:0	100:0	100:0	100:0	100:0	100:0
<b>q (Cmmol/Cmmol·h)</b>						
q <sub>TAG/X-h</sub>	0.003	0.002	0.002	0.000	0.002	0.000
q <sub>PHA/X-h</sub>	0.000	0.000	0.003	0.004	0.000	0.001
- q <sub>N/X-h</sub>	0.001	0.001	0.000	0.000	0.000	0.000
q <sub>X/S-h</sub>	0.056	0.022	0.000	0.000	0.009	0.001
<b>Y (Cmmol/Cmmol)</b>						
Y <sub>TAG/S</sub>	0.234	0.129	0.158	0.022	0.667	0.163
Y <sub>PHA/S</sub>	0.014	0.027	0.240	0.803	0.080	0.244
Y <sub>X/S</sub>	0.679	0.317	0.000	0.000	0.253	0.038

**Table 4.** TAGs and PHAs production from oily fractions using both pure culture and MMCs: a comparison with literature.

Inoculum	Feedstock	Production process	wt % max.	Y <sub>TAG/S</sub> - Y <sub>PHA/S</sub>	Reference
<b>TAGs pure culture</b>					
<i>Mucor circinelloides</i>	Cheese whey	Erlenmeyer flasks	34	0.04 g / g	Chan et al. (2018)
<i>Rhodococcus opacus</i>	Olive oil mill waste	Rotary shaker	77 – 83	-	Herrero et al. (2018)
<i>Rhodococcus Jostii</i>		Petri plates			
<i>Rhodococcus wratislaviensis</i>					
<i>Yarrowia lipolytica</i>	Pork lard	Batch bioreactor	27 – 58	-	Lopes et al. (2018)
<b>PHAs pure culture</b>					
<i>Pseudomonas mendocina</i>	Coconut oil	Fermentation	58	-	Basnett et al. (2018)
<i>Cupriavidus necator</i>	Soybean oil	Batch bioreactor	80	0.85 g/g	da Cruz Pradella et al. (2012)
<i>Cupriavidus necator</i>	Peanut oil	Fermentation	51	0.56 g / g	Pérez-Arauz et al. (2019)
<i>Ralstonia eutropha</i>	Waste frying oil	Batch fermentation	70	-	Riedel et al. (2015)
	Tallow		63		
<i>Cupriavidus necator</i>	Tuna condensate from the fish-canning industry	Batch fermentation	42	0.42 g / g	Sangkharak et al. (2020)
<i>Pseudomonas sp.</i>	Corn oil	Cultivation in a shaker	37	-	Song et al. (2008)
	Waste vegetable oil		24		
<i>Salinivibrio sp.</i>	Waste fish oil and glycerol	Batch bioreactor	42	0.32 g / g	Van Thuoc et al. (2019)

**Table 4 (Continuation)**

Inoculum	Feedstock	Production process	wt % max.	$Y_{TAG/S} - Y_{PHA/S}$	Reference
<b>TAGs MMC</b>					
Activated sludge	Soybean oil	SBR + FBR	54	-	Tamis et al. (2015)
<b>PHAs MMC</b>					
Activated sludge	Olive oil pomace	Pretreatment + SBR	39	0.36 g / L	Waller et al. (2012)
Activated sludge	Olive oil mill wastewater	Pretreatment + Acidification + SBR + FBR	30	0.56 g COD / g COD	Campanari et al. (2014)
Activated sludge (10 %) and palm oil mill effluent (90 %)	Palm oil mill wastewater	Single SBR for growth and accumulation	45	-	Md Din et al. (2006)
Activated sludge for aerobic granules formation	Palm oil mill wastewater	Pretreatment + SBR	68	0.66 g /g COD	Gobi and Vadivelu (2014)
<b>PHAs + TAGs MMC</b>					
Activated sludge	The oily fraction of a fish- canning industry effluent	SBR + FBR	<sup>(1)</sup> TAG: 43 <sup>(2)</sup> PHA: 82	<sup>(1)</sup> 0.67 Cmmol <sub>TAG</sub> / Cmmol <sub>S</sub> <sup>(2)</sup> 0.80 Cmmol <sub>PHA</sub> / Cmmol <sub>S</sub>	This research work

<sup>(1)</sup> Data concerning Period IV, highest TAGs accumulation and production yield. <sup>(2)</sup> Data regarding Period III, highest PHAs accumulation and production yield.

# **A novel strategy for triacylglycerides and polyhydroxyalkanoates production using waste lipids**

Lucía Argiz <sup>a\*</sup>, Rebeca González-Cabaleiro <sup>b</sup>, Ángeles Val del Río <sup>a</sup>, Jesús González-López <sup>c</sup>, Anuska Mosquera-Corral <sup>a</sup>

<sup>a</sup> CRETUS Institute, Department of Chemical Engineering, Universidade de Santiago de Compostela, 15782 Santiago de Compostela, Galicia, Spain

<sup>b</sup> Department of Infrastructure and Environment, University of Glasgow, Rankine Building, Glasgow, G12 8LT, UK

<sup>c</sup> Department of Microbioloy and Institute of Water Research, Universidad de Granada, Granada, Spain

\* Corresponding author: [luciaargiz.montes@usc.es](mailto:luciaargiz.montes@usc.es)

**Figure S1.** Configuration of the SBR cycles during the different operational periods (I – V).

**Coupled system configuration (period I)**

Feeding <sup>1</sup>				
Aeration				
Withdrawal				
<b>Time (min)</b>	<b>5</b>	<b>708</b>		<b>7</b>

Feeding<sup>1</sup>: 2 mL C & 2 L of a nutrients solution containing N.

**Uncoupled system configuration type A (period II)**

Feeding <sup>2</sup>				
Aeration				
Feeding <sup>3</sup>				
Withdrawal				
<b>Time (min)</b>	<b>5</b>	<b>180</b>	<b>5</b>	<b>523</b>
				<b>7</b>

Feeding<sup>2</sup>: 2 mL C; Feeding<sup>3</sup>: 2 L of a nutrients solution containing N.

**Uncoupled system configuration type B (periods III, IV and V)**

Feeding <sup>4</sup>				
Aeration				
Feeding <sup>5</sup>				
Withdrawal				
<b>Time (min)</b>	<b>5</b>	<b>120 – 180</b>	<b>5</b>	<b>523 – 583</b>
				<b>7</b>

Feeding<sup>4</sup>: 2 mL C & 2 L of a nutrients solution without N; Feeding<sup>5</sup>: 20 mL of a N solution.

**Figure S2.** Distribution of the different operational periods in the SBR (I – V) and accumulation assays performed in the FBR.

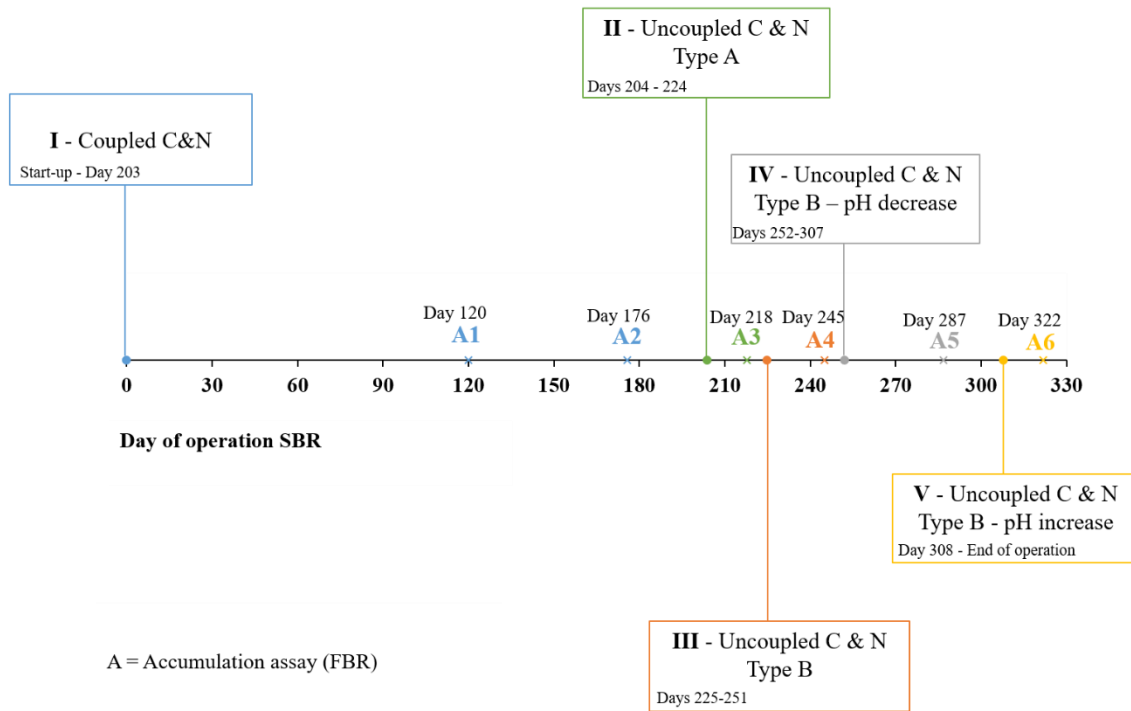


**Figure S3.** Evolution of different parameters in the SBR during periods I – V. a) Feast phase length considering accumulation + growth (○), single accumulation (●); b) Inorganic carbon (×) and pH (●) of the nutrients solution, pH at the end of the cycle (●); c) TN of the nutrients solution (●), TN at the end of the cycle (●); d) VSS at the end of the cycle (●).

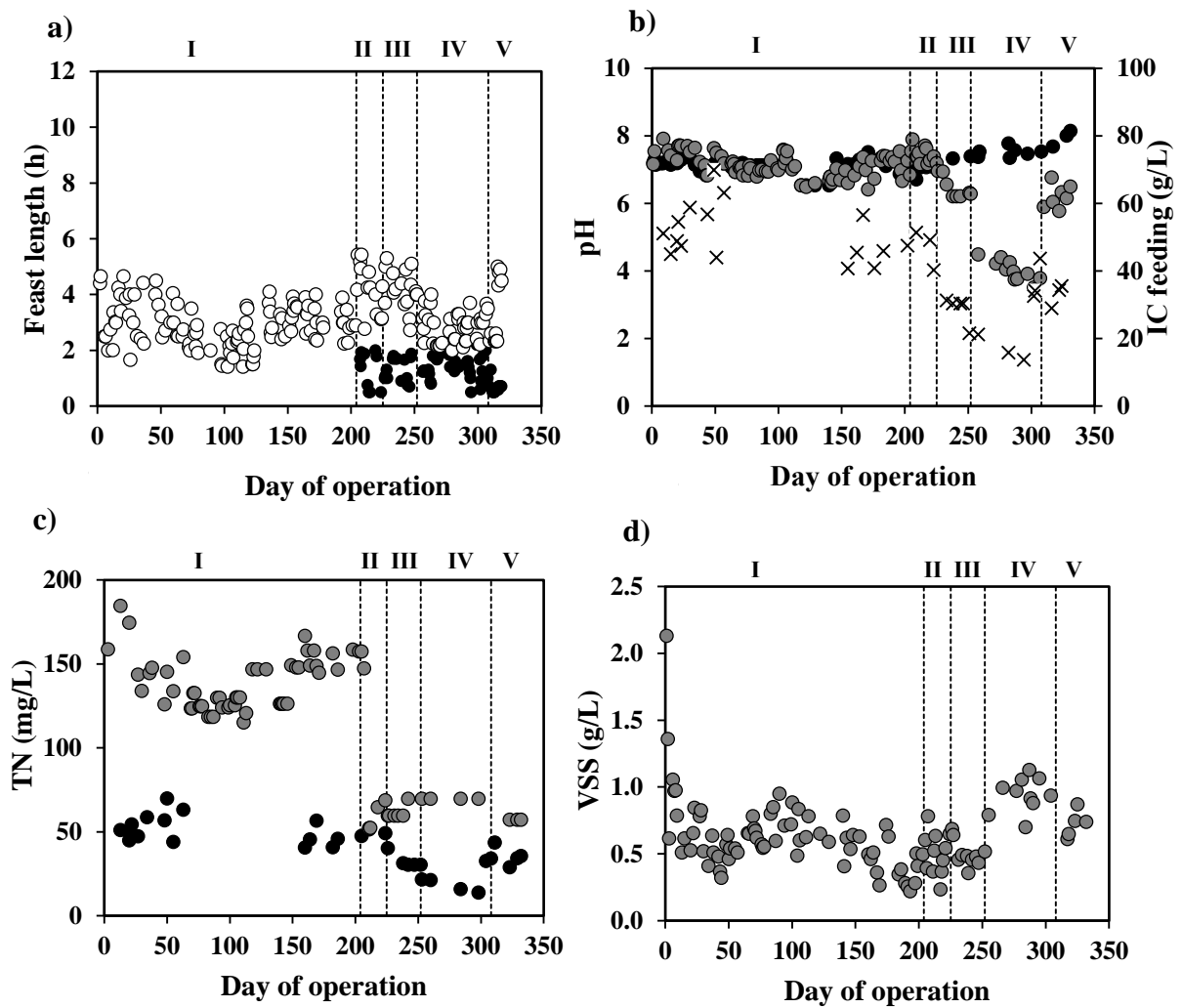


**Figure S4.** Comparison of the evolution of the dissolved oxygen (DO) profiles in the coupled and uncoupled systems and feast phase length quantification.

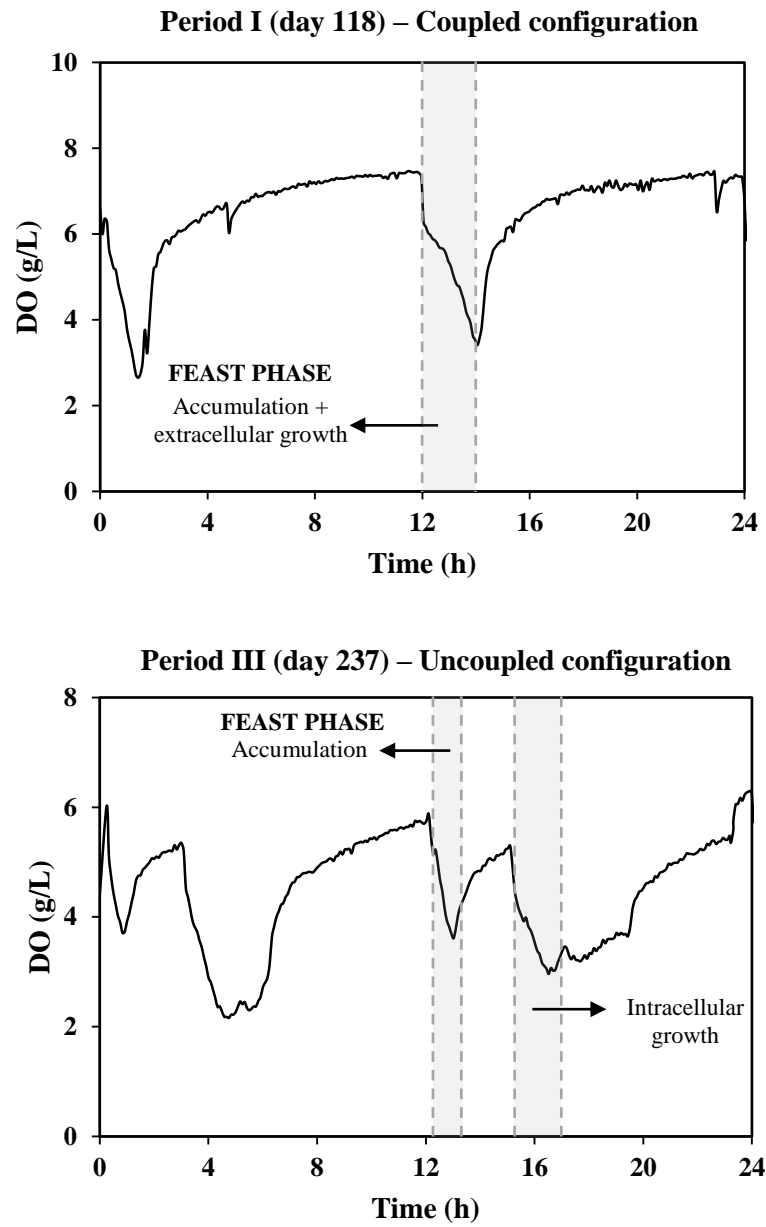


**Figure S5.** Simplified flowchart of the research methodology and operational periods.

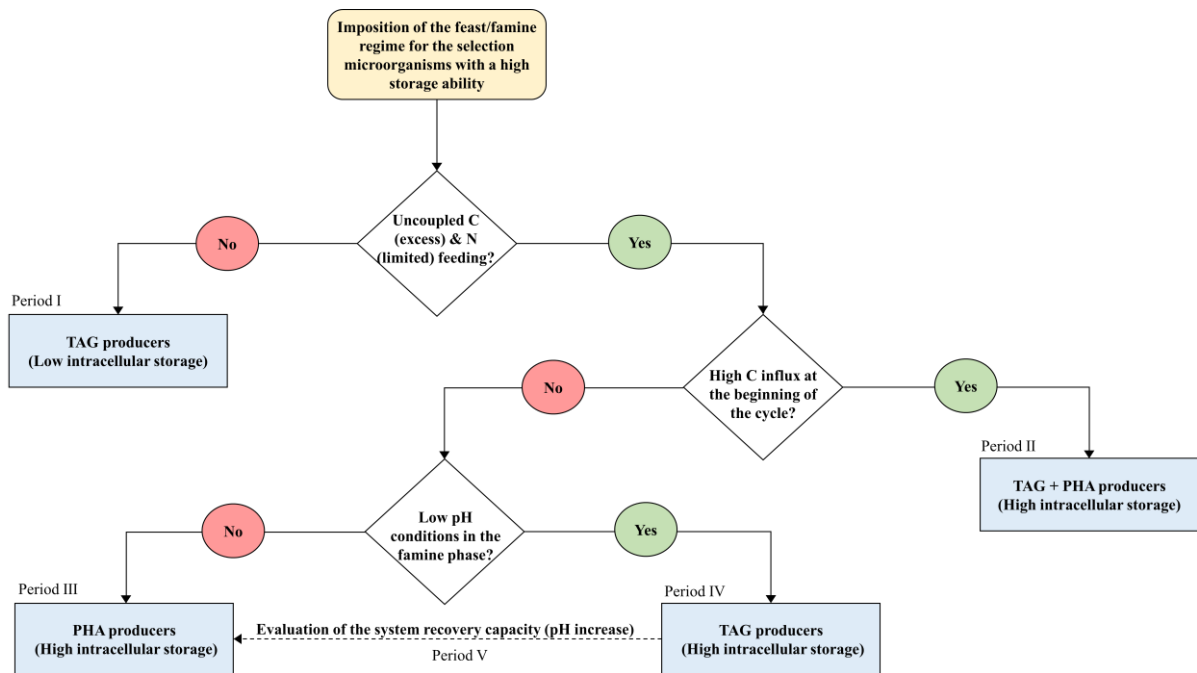


**Table S1.** Results of the statistical analysis. a) One-Way ANOVA, Turkey post hoc test considering TAG and PHA as independent variables: comparison of the storage compounds composition at the end of the feast phase in the enrichment SBR during different operational periods. b) t-test for independent samples: comparison of the composition of the intracellular compounds accumulated during the same operational periods in SBR and FBR reactors.

a)

One-Way ANOVA

		Sum of Squares	df	Mean Square	F	Sig.
<b>TAG</b>	Between Groups	11273.204	4	2818.301	8.731	.001
	Within Groups	4519.156	14	322.797		
	Total	15792.360	18			
<b>PHA</b>	Between Groups	11273.204	4	2818.301	8.731	.001
	Within Groups	4519.156	14	322.797		
	Total	15792.360	18			

Turkey post hoc tests (TAG as an independent variable)

Period (i)	Period (j)	Mean Difference (i - j)	Std. Error	Sig.	95% Confidence Interval	
					Lower Bound	Upper Bound
I	II	28.29000	14.66963	.348	-17.4197	73.9997
	III	<sup>(1)</sup> 71.51000	14.66963	<sup>(2)</sup> .002	25.8003	117.2197
	IV	-10.11000	11.59736	.903	-46.2467	26.0267
	V	26.52000	10.87929	.162	-7.3792	60.4192
II	I	-28.29000	14.66963	.348	-73.9997	17.4197
	III	43.22000	17.96655	.171	-12.7628	99.2028
	IV	-38.40000	15.55949	.154	-86.8825	10.0825
	V	-1.77000	15.03189	1.000	-48.6085	45.0685
III	I	<sup>(1)</sup> -71.51000	14.66963	<sup>(2)</sup> .002	-117.2197	-25.8003
	II	-43.22000	17.96655	.171	-99.2028	12.7628
	IV	<sup>(1)</sup> -81.62000	15.55949	<sup>(2)</sup> .001	-130.1025	-33.1375
	V	-44.99000	15.03189	.062	-91.8285	1.8485
IV	I	10.11000	11.59736	.903	-26.0267	46.2467
	II	38.40000	15.55949	.154	-10.0825	86.8825
	III	<sup>(1)</sup> 81.62000	15.55949	<sup>(2)</sup> .001	33.1375	130.1025
	V	36.3000	12.05233	.057	-.9244	74.1844
V	I	-26.2000	10.87929	.162	-60.4192	7.3792
	II	1.7000	15.03189	1.000	-45.0685	48.6085
	III	44.99000	15.03189	.062	-1.8485	91.8285
	IV	-36.63000	12.05233	.057	-74.1844	.9244

**Table S1 (continuation)**

a)

Turkey post hoc tests (TAG as an independent variable)

Period (i)	Period (j)	Mean Difference (i - j)	Std. Error	Sig.	95% Confidence Interval	
					Lower Bound	Upper Bound
I	II	-28.29000	14.66963	.348	-73.9997	17.4197
	III	<sup>(1)</sup> -71.51000	14.66963	<sup>(2)</sup> .002	-117.2197	-25.8003
	IV	10.11000	11.59736	.903	-26.0267	46.2467
	V	-26.52000	10.87929	.162	-60.4192	7.3792
II	I	28.29000	14.66963	.348	-17.4197	73.9997
	III	-43.2000	17.96655	.171	-99.2028	12.7628
	IV	38.40000	15.55949	.154	-10.0825	86.8825
	V	1.77000	15.03189	1.000	-45.0685	48.6085
III	I	<sup>(1)</sup> 71.51000	14.66963	<sup>(2)</sup> .002	25.8003	117.2197
	II	43.22000	17.96655	.171	-12.7628	99.2028
	IV	<sup>(1)</sup> 81.62000	15.55949	<sup>(2)</sup> .001	33.1375	130.1025
	V	44.99000	15.03189	.062	-1.8485	91.8285
IV	I	-10.11000	11.59736	.903	-46.2467	26.0267
	II	-38.40000	15.55949	.154	-86.8825	10.0825
	III	<sup>(1)</sup> -81.62000	15.55949	<sup>(2)</sup> .001	-130.1025	-33.1375
	V	-36.63000	12.05233	.057	-74.1844	.9244
V	I	26.52000	10.87929	.162	-7.3792	60.4192
	II	-1.77000	15.03189	1.000	-48.6085	45.0685
	III	-44.99000	15.03189	.062	-91.8285	1.8485
	IV	36.63000	12.05233	.057	-.9244	74.1844

<sup>(1)</sup> The mean difference is significant at the 0.05 level. <sup>(2)</sup> Significantly different (sig. < 0.05).

b)

Group statistics

Reactor	N° of samples	Mean	Std. deviation	Std. error deviation
SBR	5	53.0204	32.98924	14.75324
FBR	5	45.8840	35.20856	15.74575

Levene's test for equality of variances

F	Sig.
0.134	0.724

**Table S1 (continuation)**

b)

t-test for Equality of Means

	<b>t</b>	<b>Degrees of freedom</b>	<b>Sig (2-tailed)</b>	<b>Mean difference</b>	<b>Std. Error Difference</b>	<b>95 % Confidence Interval of the Difference</b>	
						<b>Lower</b>	<b>Upper</b>
Equal variances	.331	8	.749	7.13640	21.57745	-42.62130	56.89410
Equal variances not assumed	.331	7.966	.749	7.13640	21.57745	-42.65793	56.93073